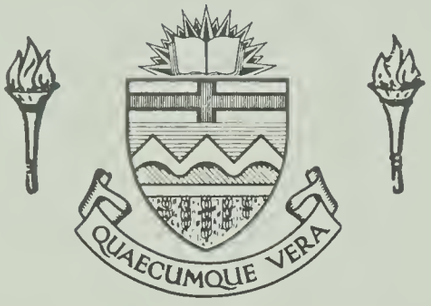

THE UNIVERSITY OF ALBERTA

RELEASE FORM

NAME OF AUTHOR ..... *Chiu Tung Chiang*

TITLE OF THESIS ..... *Behavior of Ferrocement Under Combined Tension and Compression*

DEGREE FOR WHICH THESIS WAS PRESENTED ..... *M.Sc.*

YEAR THIS DEGREE GRANTED *1979*

THE UNIVERSITY OF ALBERTA

BEHAVIOR OF FERROCEMENT UNDER COMBINED TENSION AND COMPRESSION

by

© CHIU TUNG CHIANG

A THESIS

SUBMITTED TO THE FACULTY OF GRADUATE STUDIES AND RESEARCH

IN PARTIAL FULFILMENT OF THE REQUIREMENTS FOR THE DEGREE

OF MASTER OF SCIENCE

DEPARTMENT OF CIVIL ENGINEERING

EDMONTON, ALBERTA

SPRING, 1979

THE UNIVERSITY OF ALBERTA

FACULTY OF GRADUATE STUDIES AND RESEARCH

The undersigned certify that they have read, and recommend to the Faculty of Graduate Studies and Research, for acceptance, a thesis entitled BEHAVIOR OF FERROCEMENT UNDER COMBINED TENSION AND COMPRESSION submitted by CHIU TUNG CHIANG in partial fulfilment of the requirements for the degree of Master of Science in Civil Engineering.

ABSTRACT

This study investigates the mechanical behavior of ferrocement under biaxial tension and compression. A brief review of the applications of ferrocement and a survey of the various experimental investigations are also presented. The tensile strength of ferrocement depends mainly on that of the wire mesh while the compressive strength depends mainly on that of cement mortar. Conventional reinforced concrete theory can be adopted to predict the flexural strength conservatively.

The test series consisted of ten specimens. Each specimen was loaded to failure by increasing the compression load after the designated tension load was reached. The major variables included were the specimen geometry, the amount of wire mesh reinforcement, and the value of the applied tension.

The results of the tests are presented in the form of graphs, tables and photographs. The behavior of the specimens was discussed with respect to the load-strain relationships and the cracking pattern. From the test results, it appears that there is no significant interaction between the tension and compression for the specimens tested.

ACKNOWLEDGEMENTS

The author wishes to express his sincere appreciation to Professor J. Warwaruk for his supervision, patience and valued counsel throughout the course of this work.

Funding has been provided by the National Research Council through Grant No. A1696.

The author owes special thanks to Larry Burden, Bob Billey and Watson Reid who helped in the testing program.

The author thanks Doreen Wyman for her expert typing of the manuscript.

Thanks are also due to the graduate students in the Department of Civil Engineering who helped in numerous ways.

Table of Contents

LIST OF TABLES

LIST OF FIGURES

LIST OF SYMBOLS

A	area of composite section
A_s	area of steel
A_c	area of composite
a	distance to neutral axis from extreme compression fibre
b	width of beam
d_i	distance of each mesh layer from extreme compression fibre
E	modulus of elasticity
E_c	modulus of elasticity of composite
E_m	modulus of elasiticty of mortar matrix
E_s	secant modulus of elasticity of ferrocement
e_{co}	strain corresponding to the maximum stress in the mortar constitute relationship
e_{cu}	maximum compressive strain sustained by the mortar
e_{fy}	yield strain of wire
e_{fu}	fracture strain of wire
e_{mu}	maximum tensile strain sustained by the mortar
f'_c	compressive strength of mortar
f_r	modulus of rupture of ferrocement
f_r	modulus of rupture of mortar
f_s	yield strength of wires
f_{sp}	tensile strength of concrete cylinder
M_m	ultimate moment of plain mortar beam
M_{ist}	moment at first crack
M_u	ultimate moment of reinforced beams
n	number of layers of mesh

P_m	ratio of mesh area in the stressed direction to the mortar area
S_{LT}	specific surface of reinforcement in longitudinal direction
s	average crack spacing
V_m	mortar volume ratio
V_{RL}	volume fraction of mesh reinforcement in loading direction
w	crack width
α	ratio of average compressive strength to ultimate compressive strength of mortar
β	ratio of distance of centroid to compressive stress-strain curve to distance to neutral axis
η	ratio of the interfacial bond stress to the mortar tensile stress
ν	Poisson's ratio
σ'	proof stress at 0.01% strain
σ_x	stress in the compressive direction
σ_y	stress in the tensile direction
ε_x	strain in the tensile direction
ε_y	strain in the compression direction

Chapter I

INTRODUCTION

Ferrocement, a new structural form of reinforced concrete, consists primarily of a cement-sand mortar matrix and layers of steel wire mesh reinforcement. The basic idea behind this material is that concrete can undergo large strains in the neighbourhood of the reinforcement and the magnitude of the deformations depends on the distribution and subdivision of the reinforcement throughout the mass of the concrete. As a result, when this reinforcement is subdivided into a small-diameter closely spaced mesh, the whole tends to behave as a crack-free, homogeneous material with higher tensile strength and better mechanical properties than normal reinforced concrete. Since Pier Luigi Nervi successfully proved the remarkable strength and lightness of this new method of construction, there has been increasing interest in ferrocement for both naval and civil engineering structures. Since mortar can be applied directly on the mesh, ferrocement can be fabricated to virtually any conceivable thin complex shape without forms, or with a minimum of formwork. This unique adaptability of ferrocement has led to its exploitation in boat building and structures that owe their strength to form such as thin shells and corrugated surfaces. A number of investigators have examined the engineering properties of ferrocement. Structures such as shells are basically loaded in two dimensions. However, the tests conducted are all one dimensional.

The objectives of this study are to review the mechanical properties of ferrocement investigated and to present its behavior under biaxial tension-compression. Ten ferrocement specimens were tested. The principal variables were specimen geometry, amount of wire mesh reinforcement and values of applied tension. The results were obtained in the form of electrical resistance strain gauge readings and applied load readings, and photographs of the specimens were taken after failure.

Chapter II

LITERATURE REVIEW

2.1 Introduction

Ferrocement is the name given by Dr. P.L. Nervi (1,2) of Italy, to a material consisting essentially of mortar made of fine sand and Portland cement and reinforced with a number of layers of small-diameters wire mesh to create a stiff structural form. In this chapter, ferrocement is briefly surveyed. Information on its origin, composition, present and future potential applications are reviewed. A survey of the various experimental investigations on the behavior of ferrocement reported is then presented. Much of the work has been concerned with the flexural behavior of ferrocement beams, focusing mainly on ultimate strength, cracking and deflection considerations. Little has been done on its shear strength. At present, it appears that ferrocement can be designed on the basis of conventional reinforced concrete and laws governing composite materials.

2.2 Historical Background

The ferrocement technique seems to have been first used by Lambot as narrated by Cassie (3). In 1848, Lambot constructed his first boat using cement mortar reinforced with parallel rows of steel bars interwoven in two directions at right angles. The boat and a companion one built in 1849 were afloat unnoticed in the lake at Miraval until Lambot showed his invention at the International Exhibition

in Paris in 1855. In 1955, they were rediscovered and are now housed in the museums in Brignoles and Paris. They are reported to be in good condition. Little further development was performed until Dr. P.L. Nervi (1,2) began a series of experiments on ferrocement which led to his establishment of ferrocement building technique as it is known today. In 1943, Nervi's firm began to work on three 150-ton transport boats and one 400-ton vessel. The hulls of these vessels were largely made of ferrocement. In addition to constructing the famous ferrocement vessels Irene, Toscana and Nanelle, Nervi also used ferrocement to construct several roofs which today still remain as the rational and aesthetical models in structural design.

There seems to have been little activity from 1949 to 1960. However, after the renaissance of the method in New Zealand in 1964 (4), interest in ferrocement spread to the U.S.S.R., North America, China, and eastern Europe. Though ferrocement remains largely untried, a number of investigators have examined the engineering properties of ferrocement such as suitable mix, properties of cement mortar, flexural strength, tensile strength, compressive strength, fatigue strength and water tightness.

2.3 The Material

Ferrocement is a type of reinforced concrete in which the reinforcement consists primarily of layers of wire mesh and the matrix is cement mortar. Three basic types of reinforcement commonly used are welded wire mesh, woven wire mesh and expanded metal lath. The wire diameter ranges from 0.02 to 0.06 in. (0.5 to 1.5 mm.), the

size of mesh ranges from 0.4 to 1 in. (10 - 25 mm.) and the fraction volume of mesh from 4 to 8 percent. The mesh reinforcement is distributed closely in several layers throughout the thickness of the element and is impregnated with a rich sand-cement matrix. Welded mesh reinforcements are found to be superior than other mesh types under a wide range of different types of stresses, especially drop-impact resistance, flexure strength and compression strength (18),(40), (48). Mild steel rods of about 6 mm. diameter can be inserted between mesh layers as additional reinforcement to increase the strength without losing any of the qualities of the material. It was found that rods make a significant contribution to drop impact resistance and flexural strength of mesh-reinforced panel (18).

The mortar used is composed of cement, water and fine sand which rarely exceeds 5 mm. in size and is often of 2 mm. in order to permit a more closely spaced mesh. Add mixtures such as pozzolan can be used to improve the mortar workability. The mortar is usually of high compressive strength varying from 5000 to 8000 psi (35 to 55 N/mm^2). The cement-sand ratio is of the order of 1:2 and the water-cement is kept low, usually 0.4 to 0.5, to achieve high compressive strength. The thickness of a ferrocement element is usually between 0.4 to 1.2 inches (10 to 30 mm.) and the concrete cover to the wires is usually 0.08 to 0.2 in. (2 to 5 mm.). The mortar and mesh reinforcement are considered to act largely independent of each other. The degree of homogeneity depends on the specific surface of wire mesh. The specific surface of reinforcement is the total surface area of wire in contact with the mortar divided by the volume of the composite. Bezukladov (8) suggested that for a specific surface around 5.1 $in.^{-1}$ (0.2 $mm.^{-1}$),

the material can be treated as a homogeneous material. For a specific surface less than 1.3 $in.^{-1}$ (0.05 $mm.^{-1}$), the material is considered to be reinforced concrete.

2.4 Applications

Early application of ferrocement seems to be in boat building (6-23). There is a good amount of literature available on ferrocement boat building technique and its advantages over boats constructed with reinforced concrete, steel and timber. Reduction in cost up to 40% and in weight up to 5% compared to conventional timber boats were reported by Nervi (1,2). A comparative cost analysis of ferrocement boats is discussed by Hagenbach (7), Fraser (14) and Shaw (34). The total cost of a ferrocement boat compared favourably with other materials. There is a saving in basic building materials, namely steel and cement, since it is possible to cast very thin sections with ferrocement. Formwork can be minimized or eliminated because the basic mesh can be bent by hand into required shapes and mortar is usually applied directly on to the wire mesh.

Since the reinforcement is finely distributed throughout the section, only very fine cracks are developed under service loads. It is leak-proof. Other advantages include higher resistance to impact, corrosion, better vibration-damping qualities, better fire resistance, minimum maintenance and easier to repair. In various countries around the world, both the amateur and professional boat builder have produced large numbers of apparently trouble free small craft. Lloyds Register of shipping in United Kingdom and Ministry of Transport in Canada have laid down certain regulatory aspects for the construction

of ferrocement vessels (12,14). After the report by Kelly and Mouat (6) to the Conference on Fishing Vessel Construction Materials in Canada, 1968, the Canadian Industrial Development Branch embarked on the funding of the five annual programs at B.C. Research to evaluate ferrocement for fishing vessel construction (14-18). In 1967, the Food and Agriculture Organization of the United Nations began to investigate the possibilities of ferrocement as a boat building material and the first seminar on Design and Construction of Ferrocement Fishing Vessels was held in Wellington, New Zealand on October 1972 (20). Prestressing techniques has been tested with success for ferrocement vessels in New Zealand (23).

The first application to Civil Engineering structures was made by Nervi and Baroli (1) in 1947 in the construction of an experimental storage shed for their own use. Many impressive and noteworthy applications to buildings were later made by Nervi (1,2). At that time large corrugated shells of 100 m. span were built with prefabricated ferrocement elements in the central hall and the perimeter roofs of Hall C in Turin, Italy. It offered good appearance, good thermal and sound insulation and low weight prefabrication. Because of their light weight, undulated beams of ferrocement are particularly well suited to build cantilever structures by means of prefabricated elements. Such cantilevered roofs were used in Milan Fair building in 1953.

Present applications and research effort seem to be centred in the U.S.S.R. and Eastern Europe. Khaidukov (24) describes in detail different types of ferrocement structures such as folded plate, wavy roofs and shells of single and double curvature. From 1957 to 1968, over 300,000 sq.m. of ferrocement roofs and many other space structures

was reported to have been constructed in the U.S.S.R. Apart from the advantages of light weight, ferrocement is claimed to have a 15 - 25% saving in steel consumption and a 10% saving in roof costs. Because of the large number of small diameter wires, reinforcement in ferrocement has about 10 times as much specific surface area as conventionally reinforced concrete (5). This results in a considerably increased bond strength. Consequently, ferrocement can be made to have high tensile strength and cracks are very small even at failure. Therefore, the need for waterproofing can be eliminated. Because of its high extensibility, ferrocement is specially suitable for hanging roofs.

In Eastern Europe, ferrocement is being used in the lining of mining shafts and tunnels, as well as for water proofing and decorative cover (30). Ferrocement also suits well to those structures that owe their strength to form such as thin shells and corrugated surfaces.

Ferrocement has also been used or suggested for use for grain-storage silos, railroad ties, storage tanks of water, milk and liquid gases, buoys and deep submersibles (25). It has been suggested as a possible building material for developing countries, especially for roofing of housing construction (26, 27). Other potential applications of ferrocement which take advantage of the high tensile strength to weight ratio and watertightness include ferrocement shelter, sandwich panels for housing and permanent forms for concrete columns (28).

2.5 Experimental Investigations

2.5.1 General

Since Nervi's work, research on ferrocement as an engineering material has been steadily increased. Its mechanical properties in

uniaxial tension and compression, flexure, impact and fatigue have been investigated by several researchers (30-55). A survey of investigations on ferrocement was reported by G.W. Bigg (16) in 1972, and ferrocement as a composite material was also discussed. Guidelines for analysis and design of ferrocement elements were presented based on available knowledge. There are many variables which affect the quality of finished ferrocement, namely mix design, water-cement ratio, type and amount of mesh, mixing and curing conditions, etc. At the present state, no standard tests have been established for predicting the design strength and stiffness data. Elastic constants such as the modulus of elasticity (16,37,38,44), the modulus of rigidity (37) and Poisson's ratio (37) have been investigated, but no agreed values have been determined. Currently it appears that ferrocement can be designed on the basis of conventional reinforced concrete theory and laws governing composite materials. The engineering properties of ferrocement do not appear to have reached a conclusive stage.

2.5.2 Tension Test Results

Ferrocement has considerable tensile strength because of the closely spaced mesh reinforcement. However it still cracks at relatively low stresses. There are two major classes of failure of interest:

(a) ultimate rupture and elongation of element,

(b) the influence of percentage and dispersion of reinforcement on the development of first crack.

Walkus (31) studied the behavior of ferrocement under axial tension, the state of cracking, the relation between cracks and specific surface of reinforcement. He concluded that ferrocement differs from

reinforced concrete by its relatively high specific surface ratio ($> 0.8\ cm^{-1}$). A tensile stress-strain curve for ferrocement was proposed. Cracking behavior in relation to crack width was also presented. The stress-strain curve was divided into five phases according to the crack width, namely, linearly elastic, quasi elastic, nonlinearly elastic, elastic plastic and plastic.

Bezukladov (8) claimed that the ultimate tensile strength of ferrocement is a function of the steel alone and that the stress to initiate cracking is higher in mesh samples. He noted that the higher the specific surface, the lower the width of cracks.

Naaman and Shah (32) studied the influence of type, size and volume of wire meshes on elastic, cracking and ultimate behavior of ferrocement in uniaxial tension. It was observed that the ultimate tensile strength of ferrocement was the same as that of the mesh alone. This is in agreement with the conclusion of Bezukladov (8). The modulus of elasticity of ferrocement can be estimated using the law of mixture of composite material. For the uncracked state,

$$E_{c1} = (1 - V_{RL})\, E_M + V_{RL} E_{RL} = E_M + V_{RL} E_{RL} \qquad (2.1)$$

where E_{c1} is the modulus of elasticity of ferrocement for the uncracked stage, E_M is the modulus of elasticity of the mortar matrix, E_{RL} is the apparent modulus of elasticity of mesh in the loading direction and V_{RL} is the volume fraction of reinforcement in the loading direction. For the cracked stage, the modulus of elasticity can be estimated as:

$$E_{cz} = E_{RL} V_{RL} \qquad (2.2)$$

This prediction gave lower bound values.

Increasing the specific surface of reinforcement increases the stress at the onset of cracking, the number of cracks to failure, the toughness and the elongation at ultimate load. Stress at first cracking increased linearly with increase in specific surface irrespective of size, type and spacing of wire mesh. An analytical relation between average crack spacing and the specific surface of reinforcement was developed. The theoretical crack spacing was found to be as follows:

$$S = \frac{1.5}{\eta} \frac{1}{S_{LT}} \tag{2.3}$$

where $\eta = 1.6$. With higher specific surface, the crack spacing decreased resulting in smaller crack widths. Woven mesh with the angle of weave greater than 0.12 and chicken wire mesh were found to be unsatisfactory because premature mortar spalling of mortar matrix was observed before the maximum tensile stress was reached.

A leakage test on ferrocement was reported by Shah and Key (33,35). It was observed that the average number of cracks at failure varied linearly with increase in specific surface ratio. The width of cracks at failure depends also on the yielding characteristics and ultimate strength of steel. The use of different types of sand did not influence the tensile strength of ferrocement.

Desayi and Jacob (36) confirmed the findings of Shah that the ultimate tensile strength of ferrocement was equal to that of mesh alone, and that the spacing of cracks decreased with increase in the specific surface of reinforcement.

Direct tension tests on ferrocement specimens with different number of layers of galvanized hexagonal wire mesh and reinforced with 6 mm. diameter mild steel bars were performed by Pama, Sutharatanachaiyaporn and Lee (37). Theoretical modulus of elasticity and ultimate loads developed from the law of mixtures were found to be in good agreement with experimental results. The ultimate tensile strength was controlled by the strength of wire mesh only, with no contribution from the skeletal steel due to premature bond failure.

Nathan and Paramasiva (38) showed that the tensile first crack stress was proportional to specific surface of wire mesh only if the proof stress correspond to 0.01% strain for the various steels used was approximately the same. The cracking behavior of ferrocement was influenced by the total bond stress between steel and mortar. The number of cracks at failure was also influenced by the specific surface and proof stress of steel. For a given steel, the number of cracks increased with an increase in the specific surface of steel. Ductility of ferrocement material increased with an increase in the percentage of reinforcement.

The effect of thickness of specimen on the stress at first cracking is very small (39). Experimental tensile modulus of elasticity was found to be independent of thickness of mesh, methods of determination and size of mesh, and agreed with the theoretical value developed from the law of mixtures. Hence, ferrocement was claimed to be an homogeneous material. For low percentage of reinforcement, the following expressions can be used in predicting modulus of elasticity and first crack stress in axial tension respectively.

$$E_c = E_c (A_s/A_c) + E_M \quad (2.4)$$

$$\sigma'_c = \sigma'_s (A_s/A_c)^{1.1} + \sigma'_m \quad (2.5)$$

Johnston and Matter (40) investigated the effect of specimen thickness, amount and orientation of mesh reinforcement on unaxial tensile strength, efficiency ratio as well as deformation, cracking and failure in tension. Their findings were as follows:

(1) The tensile strength of ferrocement is independent of the thickness of the mortar and largely reflects that of the reinforcement.

(2) Orientation of the reinforcement has a marked effect on tensile strength and on the relative efficiency of expanded metal and welded mesh.

(3) Expanded metal and welded mesh in their normal orientations offer approximately equal strength which is about 10% to 20% more than expected for the steel alone.

(4) Expanded metal is superior for uniaxial loading, but is weak in the secondary direction. Welded mesh offers equal strength in both directions, with some weakness on 45° plane.

(5) The stiffness of specimens reinforced with expanded metal is significantly greater than that of specimens having an equal area of welded mesh. The stiffness of ferrocement is largely dependent on the geometry and ductility of the reinforcement and is independent of the steel strength.

(6) The average visible crack spacing decreases as the specific surface of the welded mesh reinforcement increases in the same

manner as observed by Naaman and Shah.

(7) Steel strength is not an important parameter. Specimens with expanded metal exhibit virtually no visible cracking until just before failure. It was concluded that the geometry of the reinforcement and the material characteristics of the steel govern the load-strain and cracking behavior.

2.5.3 Compression Test Results

The mode of failure of concrete in compression is either a splitting failure due to tensile strains generated by the Poisson's ratio effect or by a shear failure. The compressive strength of mortar used in ferrocement is usually in the range of 5000 to 8000 psi (35 to 55 N/mm^2). Studies by Kelly and Mouat (6), Bezukladov (8), Rao and Gowder (41), Lee (37) and Johnston (40) show that the compressive strength of ferrocement depends primarily on that of cement mortar. The specific surface or volume of reinforcement has no significant effect because at failure, mortar splits longitudinally and mesh buckles. There is some increase in the ultimate compressive strength with increase in steel content (40,41). However, after about 2 percent reinforcement, the ultimate compressive strength remains almost constant. Steel strength and orientation of mesh reinforcement seem to be of little effect (40). Instead, the geometry of reinforcement has a marked effect on strength. Johnston found that lateral reinforcement influences strength much more strongly than longitudinal reinforcement (40). The lateral steel in the square welded mesh can carry 17% - 42% of the load. Therefore welded mesh is much superior to expanded metal as compression reinforcement as it can provide lateral confinement of the mortar.

The behavior of ferrocement under compression is similar to that of ordinary reinforced concrete (41). The modulus of elasticity of ferrocement in compression is directly dependent on those of mortar and meshes, and on volume of reinforcement. Elastic behavior of ferrocement in compression can be predicted by using the law of mixtures (37). Poisson's ratio decreases with increasing volume fraction of the wire mesh.

Rao (41) concluded that smaller diameter wire mesh would be preferable to use as this gives higher elasticity and higher ultimate compressive strength for the same percentage of reinforcement with all other factors remaining the same. Provision of reinforcement in excess of about 2 to 2.5% is uneconomical as the proportional increase in strength is not achieved.

2.5.4 Impact Test Results

The extent of local damage due to impact loads on ferrocement is of direct concern in its marine applications. Nervi (1) conducted impact tests by dropping a weight of 2.45 KN. on to ferrocement samples of 30 mm. thick from different heights. He showed that failure was not characterised by the appearance of a hole, but by a widely dispersed area of shattered mortar. The material remained impervious and in a cohesive state at failure.

In Kelly's (6) test, impact resistance of ferrocement panels was less than expected. The failure for panels with 2 to 4 mesh layers was by cracking at comparatively low loads while that for panels with six or more mesh layers was by punching shear at higher loads.

Bezukladov (8) showed that there was a significant increase in energy absorbed from falling weights when specific surface of wire mesh was increased. The crushed concrete was held back by the mesh from disintegrating. However, there was a law of diminishing returns in effect in that the improvement to impact strength was lessened when more layers of mesh were used.

Greenius (15) studied the influence of rod-mesh reinforcement on impact loading. Three types of mesh, namely, 1/2-19 gage hardware cloth, 1/2-16 ga. welded square mesh and 1/2-22 ga. hexagonal mesh were used in equal amounts. The panel containing 1/2-19 ga. hardware cloth showed better impact resistance. It was found that provision of rod reinforcement improved the strength under impact. Steel rods served to prevent extensive propagation of open cracks. The panels tested showed no visible cracking in the top impact surface. Fine radial and rectilinear cracks were observed in the bottom surface.

Shah and Key (34) studied the influence of specific surface and yield strength of wire mesh on impact resistance by measuring the rate of flow of water through a ferrocement panel after it was subjected to impact load. The impact loading was applied with the double pendulum method. It was concluded that the higher the specific surface of reinforcement, or the higher the yield strength of wire mesh the lesser the leakage rate and therefore the lesser the damage due to impact loading.

Nathan and Paramasiva (38), using the pendulum method, showed that the impact failure of ferrocement was confined to area of impact and crack propagation was localised due to good crack arresting mechanism. This property improved and the energy absorbed increased

with an increase in the percentage volume of reinforcement.

Chang (43), from his dynamic tests on ferrocement beams, found that when subjected to impact loads, no large fragment fell out from the specimen. The multiple layers of mesh held the fragment together. Greater deflection than similar conventional reinforced concrete beams was observed. This indicated that larger energy could be absorbed and ferrocement performed well in resisting dynamic loads.

2.5.5 Bending Test Results

Bending tests involving simply supported beams with point load at the centre were performed by Collen (42) and Rao (44). This type of loading involved bending and transverse shear. Bending tests reported by other investigators (37,38,46-52) involved third point loading which subjected a section to a constant bending moment without shear.

Collen (42) investigated the effect of steel content on ultimate bending stress, shear stress and modulus of elasticity. The tests showed that the ultimate bending and shear stresses and the modulus of elasticity increased with increase in steel content. The effects of variations in cement-sand and water-cement ratios on ultimate bending stress were demonstrated. A maximum stress was reached with cement-sand ratio of 0.66 for a water-cement ratio of 0.56. The water-cement ratio was more critical because there was quite an appreciable drop in strength as the water content was increased. A ratio of 0.35 was used so as to provide a workable mix in the tests.

Chang (43) presented an inelastic analysis of flexural behavior of ferrocement beams by assuming that the panels behaved similarly to

concrete beams with layers of closely spaced steel bars. Moment-curvature and load-deflection relationships for static and dynamic loads were developed. It was found that ultimate capacities and deflections predicted by the theory were less than test results. Fine cracks were observed in the tension zone at the early stage of flexure loading. Results from dynamic tests were also discussed.

Muhlert (44) carried out bending tests on ferrocement beams. The behavior of ferrocement in bending follows the normal load-deflection curve for reinforced concrete. These tests showed that the flexural theory of reinforced concrete members can be applied to ferrocement elements under working loads as well as ultimate loads, although the theoretical predictions were conservative.

Rao and Gowder (45) studied the influence of percentage of steel reinforcement and size of mesh on the ultimate flexural behavior. The results showed that the ultimate bending strength increased with increase in steel percentage. Modulus of elasticity increased in direct proportion with steel percentage. This agreed with Collen's result. For the same steel content, modulus of elasticity and bending strength were slightly greater when smaller diameter wires were used. The extensibility was found to increase with the percentage of reinforcement.

Desayi and Jacob (36) observed a definite correlation between the flexural strength of ferrocement and a non-dimensional quantity termed as mesh-mortar parameter, $P_m f_s / f_c$. This parameter took into account the proportion of mesh wires in the direction of stressing, and the strength properties of wire and mortar. Theoretical ultimate

moment was computed based on the following assumptions:

(a) The mesh reinforcement is uniformly distributed over the entire depth of the section and mesh wires are stressed to f_s in compression and tension at ultimate.

(b) The flexural compressive stress distribution in mortar at ultimate is rectangular with a height equal to 0.68 times the 10 cm. side cube strength.

(c) Tensile strength of mortar is negligible.

This method underestimated the tested ultimate moment by about 24 percent. The variation of modulus of rupture treating ferrocement as a homogeneous material behaving elastically up to failure was plotted against mesh-mortar parameter. It was found that the presence of mesh increased the modulus of rupture of ferrocement. Proportional increase in modulus of rupture due to mesh $(f_r - \bar{f}_r)/\bar{f}_r$, increased with the mesh parameter. Logan and Shah (46) studied the influence of volume and specific surface of reinforcement on flexural behavior of ferrocement beams. It was found that increasing the specific surface area of mesh reinforcement increased the moment at first cracking and the number of cracks to failure, but decreased the crack width for a given steel stress. The first cracks were about 0.0003 in. wide. The following equation for moment at first crack in lb. in. units was obtained:

$$M_{ist} = 400\, S_{LT} + M_m \qquad (2.6)$$

The average crack spacing at failure decreased with increasing specific surface. The maximum crack width for ferrocement could be

predicted knowing the maximum steel stress and the specific surface of the reinforcement.

Logan and Shah defined the cracking moment as those relating to the occurrence of certain crack width. Rajagopalan and Parameswaran (47,48) analysed Shah's result on the assumption that at the cracking stage, the extreme edge in the tension zone of the mortar matrix reached its peak strain e_{mu}. The ferrocement beam was assumed to comprise of a ferrocement pack in the tension zone only. The strain-space relationship was assumed to be linear. The stress-space relationship in the compression mortar was linear while that in the tension zone was parabolic. Computations of cracking moment assuming cracking strains of 200 and 300 microstrains, were presented. It was found that predictions compared well with the experimental values obtained by Logan and Shah. In developing the relationship between average crack spacing and specific surface, Logan and Shah neglected the effect of the mortar volume ratio, V_m. Rajagopalan and Parameswaran modified the expression as follows:

$$s = \frac{1.5\ V_m}{n\ S_{LT}} \qquad (2.7)$$

where n was the ratio of the interfacial bond stress to the mortar tensile stress, and was taken to be 1.6 by Shah.

It was observed that the relationship between the average crack spacing at failure and the specific surface for uniaxial tensile case also applied to beams under bending.

Logan and Shah used similar procedures in the ultimate strength design of conventionally reinforced concrete beams to predict the

ultimate strength of ferrocement beams. The strain in the top compression mortar fibre at ultimate was taken as 0.005 and strains were assumed to be linearly distributed. For an assumed value of the depth of neutral axis, an equilibrium check was made. The ultimate moment for a correct value of a was calculated as

$$M_u = \alpha f_c' ba(a - \beta a) + \sum_{i=1}^{n} A_s f_{si} y_i \qquad (2.8)$$

where $y_i = d_i - a$

$\alpha = 0.7$

$\beta = 0.4$

Rajagopalan and Parameswaran used three strain regimes to compute the ultimate moment of a ferrocement beam. Strain regime I denoted failure that occurred by the mortar strain in the extreme compression edge reaching the value of maximum compressive strain and the fibres in the tension zone being above the yield strain, e_{fy} but below the fracture strain, e_{fu}. All fibres yielded and reached their yield stress, f_s. Strain regime II was assumed to occur when the failure was governed by the mortar reaching its compressive strain, e_{cu} while the strain in the fibres in some layers remained below the yield strain and the remaining fibres yield but do not fracture. Strain regime III denoted the failure that the extreme layer of fibres had reached the fracture strain and the strains in all other fibre layers are above the yield strain, but the compressive strain at the extreme edge is less than e_{cu}. Expressions was derived and segments of computer program were written. The program first

examined the beam in regime I and control was transferred to the appropriate segment according to the fibre strains. The expressions were used to analyze and compare with test results by Rao and Gowder (45), and Logan and Shah (46). In the case of beams of Rao and Gowder, assuming e_{mu}, e_{co}, e_{cu} and e_{fu} being 300, 2000, 4000 and 30,000 microstrains respectively, the average ratio of M_u(Expt.)/M_u(Calc.) was 0.99. In the case of Shah's beams, e_{mu}, e_{co}, e_{cu} and e_{fu} were assumed to be 300, 3000, 5000 and 10,000 microstrains. The average ratio of experimental ultimate moment to predicted ultimate moment of beams was 1.05 while that computed using Shah's approach was 1.27. It can be concluded that the expressions derived for ultimate strength give good correlations with experimental results.

Johnston and Mowat (49) investigated the influence of mortar strength, plank thickness and amount, orientation, type and yield strength of reinforcement on strength of ferrocement in bending. Their findings were as follows:

(a) The strength of mortar, whether lightweight or normal weight is relatively important. A strength of 5000 to 7000 psi was recommended to compromise between adequate strength and excessive shrinkage.

(b) Orientation of mesh has a marked effect on the flexural strength of ferrocement beams reinforced with expanded metal and welded mesh. The steel elements in the expanded metal made an angle of 22° or 68° with the direction of applied stress. It was found that strength in one direction was only about 13% of that in the other. The effect was scarcely discernible with woven mesh.

(c) Plank thickness was of little importance in the beams investigated.

(d) The performance of different type of reinforcing systems of the same yield strength is strongly influenced by their geometry and method of manufacture. For any given effective cross-sectional area of steel, expanded metal and welded mesh in their normal orientations performed significantly better than woven mesh or standard bars even when bond failure was artificially prevented in the latter reinforcing systems. For any given steel content, the order of performance for uniaxial bending is expanded metal, standard bars, welded mesh and woven mesh. In terms of biaxial bending, welded mesh offers good performance in both directions and is more effective than woven mesh and expanded metal which is weak in the second direction.

(e) Steel yield strength is of relatively minor significance on the flexural strength of ferrocement.

(f) A computer program based on ultimate load analysis was used to calculate the ultimate moment. The efficiency ratio which is the ratio of actual to calculated ultimate moment was found to be affected by the orientation and specific surface of reinforcements. For a given steel percentage, smaller wire diameter and therefore higher specific surface resulted in a higher efficiency ratio.

(g) For any given steel content, performance was optimal when the reinforcing layers were spaced uniformly throughout the depth of the section.

Lee (37) performed bending tests on simply supported beams which were subjected to third-point loading. It was concluded that the

load-deflection curve could be approximated by three linear ranges, namely the uncracked, the cracked and the yield ranges. The specimens were reinforced with hexagonal wire mesh and 6 mm. steel bars. In the uncracked range, ferrocement could be treated as a homogeneous isotropic composite elastic material, and strength could be determined from the law of mixtures. The presence of wire mesh did not influence the flexural strength but increased the resistance of the mortar to crack propagation. It was observed that cracks coincided with the diagonal segments of the wire mesh.

Nathan and Paramasiva (38) observed that there was reduction of modulus of rupture when the percentage of reinforcement was more than about 3%. As the amount of reinforcement increased, the bonding between the mortar and the wire mesh decreased due to poor compaction. An expression for moment at first cracking was derived by assuming that homogeneity and law of mixtures of composite material were applicable (39). The predicted values gave lower bound results. Kumar and Sharma (50) designed a two-point loading arrangement so that load could be applied in the upward direction and crack width could be conveniently measured. The behavior of ferrocement in bending from ultimate strength, cracking and deflection considerations was studied. Theoretical ultimate moment capacity of ferrocement section was calculated using the conventional reinforced concrete theory. The distribution of strains across the section was shown to be reasonably linear. It was found that the reinforced concrete theory gave a conservative prediction. No definite variation of moment values on crack widths was observed from varying the specific surface

ratio and percentage of reinforcement. The stage at which cracking occurred, with respect to the ultimate state, was delayed considerably in ferrocement when compared to reinforced concrete. The strain readings measured with a demec gauge at 6 mm. from the extreme tensile fibre were assumed to represent the strain in the extreme wire mesh layer. A linear variation between maximum crack width and steel strain in extreme wire mesh layer was observed. From the central deflection values, it was concluded that as the steel content increased the deflection limit for the material might be increased.

In 1976, Kumar and Sharma (51) performed another bending test series on ferrocement. Two types of loading arrangement were used, namely, a uniformly distributed loading and a two-point loading. It was concluded that conventional reinforced concrete theory could be adopted for predicting the ultimate flexural strength of ferrocement until a more reliable theory is available. The ultimate strength and first crack strength were found to increase linearly with increases in the percentage area of reinforcement. On treating ferrocement as a homogeneous material, the ultimate strength and the first crack strength could be expressed in terms of the extreme fibre stress and linear relationships were obtained. Difference in steel strengths would not affect the first crack strength of the ferrocement specimens.

Ferrocement beams reinforced with different types and amounts of meshes were tested under montonically increasing four-point loading by Balaguru and Shah (52) to study the cracking behavior under bending. The load-deflection curves were observed to have three distinct stages:

(a) before cracking of mortar,

(b) after the first crack of mortar but before yielding of steel,

(c) after yielding of steel meshes.

The transverse wires of the outermost layer of mesh were preferential locations for cracks. Generally, the total number of cracks equalled the number of transverse wires and was reached soon after the first cracking load. Everything else being equal the average crack spacing was generally larger for specimens reinforced with the 1/2 mesh than for those with the 1/4 mesh. For the same stress in the outermost layer of steel mesh, the ascending order of average crack width of the specimens was those reinforced with 1/4 mesh, 1/2 welded mesh and 1/2 woven mesh. The specific surface of reinforcement did not seem to influence the cracking behavior in flexure as in tension. This was because in bending, the specific surface of the tensile zone of mortar around the outermost layer of mesh does not vary proportionally to the number of mesh layers used. Using the actual stress-strain properties of the mortar and mesh, a computerized nonlinear analysis model was developed to predict the moment-curvature and load-deflection relationships of ferrocement beams. Fourier series was used to represent the stress-strain curves of mortar and mesh. Predictions compared well with tested results. The calculated values of mortar compressive strain on the extreme fibre at the ultimate moment varied substantially with the type and number of mesh layers used, and was quite different from the recommended value of 0.003 for reinforced concrete elements. A regression analysis of observed crack widths showed that the average crack width was primarily a linear function of the strain in the extreme layer of tensile steel, and did not seem to depend on other parameters found important for reinforced

concrete. This results because of the relatively small cover and the high specific surface of ferrocement beams. A simple equation was proposed to give upper bound values of average crack width as a function of the steel strain in the outermost layer, e_s, as follows

$$w = e_s S_T R \tag{2.9}$$

where w is the calculated crack width, S_T is the spacing of the transverse wires and R is ratio of distances to neutral axis from extreme tension fibre and from centroid of steel.

2.5.6 Fatigue Test Results

Although fatigue strength may be a criterion for the design of ferrocement boat hulls and water tanks due to repeated loadings on the structures, there is little information available on the fatigue strength of ferrocement.

Picard and Lachance (53) performed preliminary fatigue tests on ferrocement plates reinforced with electric welded wire mesh and deformed steel rods. The plates were subjected to bending by applying a concentrated load at their centres. It was found that the maximum load causing failure at 1,000,000 cycles was approximately 46% of the ultimate static load. Most fatigue fracture in the wires took place at welded joints.

McKinnon and Simpson (54) studied the effect of various fabricated ferrocement subjected to constant amplitude cyclic loads up to ten million cycles. It was concluded that the ungalvanized welded square wire mesh imparted greater fatigue strength than galvanized wire mesh. The influence of curing methods, namely water-curing and

steam curing, and wire type on the fatigue strength of expansive cement and Portland cement Type 5 mortar was studied. It was found that for a 0.45 water/cement ratio, only the water-cured expansive cement with galvanized mesh reinforcement had better fatigue strength than the similarly fabricated Portland cement Type 5 specimens. There was no significant difference in fatigue strength between expansive mortar and Type 5 mortar for the same curing method and same type of reinforcement.

Karasudhi, Mathew and Nimityongskul (55) investigated the effects of the types of wire mesh on the fatigue strength of ferrocement. It was concluded that chicken wire mesh imparted greater resistance to fatigue than welded square mesh and expanded metal. The fatigue strength of ferrocement was found to depend on the fatigue properties of wire mesh.

2.5.7 Shear Test Results

Experimental results for the tests of shear strength are scarce. Kelly and Mouat (6) performed some transverse shear tests and found that the shear strength varied linearly with the number of layers of mesh. Ferrocement is not strong in transverse shear and in-plane shear was assumed by Bezukladov (8) as 1420 psi (10 N/mm^2).

2.5.8 Miscellaneous Test Results

Tests for extensibility of ferrocement elements were carried out by Oberti (1). The effects of steel contents on the elongation at failure was studied. For wire mesh up to 12.5 lb/cu.ft. (1.96 KN/m^3), the extensibility increased by about five times that of unreinforced mortar.

Results of tests on ferrocement panels from Lloyds Register of Shipping was reported by Thomas (12). These included the tests for ultimate bending tensile strength, ultimate direct tensile and compressive strength, bending fatigue and thermal conductivity. Other physical properties of ferrocement were also presented.

Beginning 1969, the British Columbia Research Council conducted a five-year program to determine the properties of ferrocement (14 - 18). Greenius and Smith (14) reported that no clear relationship could be observed between the bond area and ultimate bending stress of panels with different meshes. The influence of various mortar admixtures and rod-mesh reinforcement configurations on flexure, impact and durability (freeze-thaw and seawater exposure tests) was studied (15). It was found that provision of rod reinforcement along with mesh reinforcement improved the strength and deformability characteristics under flexure and impact. Ferrocement with welded wire mesh exhibited superior strength compared to other mesh types. A mathematical model of analysis of bending in working stress range was derived using conventional reinforced concrete theory. The models predicted the strengths of ferrocement elements conservatively. Ferrocement as a composite material was discussed by Bigg (16). A survey of investigation, guidelines for analysis and design of ferrocement were presented. The behavior of ferrocement under cyclic flexural loads and under the stress imposed by bolted fastenings, the resistance of a variety of paint coatings under various exposure conditions, and the need for control of internal quality were presented by Greenius (17). Test results and conclusions from the program were presented in Reference 18.

Tekal Viswanath (56) reported a full scale test of ferrocement precast folded plate reinforced with galvanized square mesh and mild steel bars. The folded plate was trapezoidal in cross-section and was jointed at folds from precast ferrocement plate elements. It was found that the major contribution to deflections was caused by flexure. The deflections caused by transverse slip and shear were found to be 2% and 3.5% respectively. The test unit failed in shear along the folded line joints at the diaphragm.

Gopalakrishnan (57) conducted tests on three ferrocement folded plate specimens. The tests showed that the theoretical ultimate moment and deflection under working load calculated on the basis of equivalent beam section agreed well with the test results.

Desayi and Joshi (58) conducted tests on undulated ferrocement wall specimens to determine the influence of slenderness ratio and the amount of reinforcement. It was found that the specimens behaved like short columns up to a slenderness ratio of 38. For the range of mesh used, the ferrocement plates had an average compressive strength of about 83% of the mortar cube. Methods suggested for the design of reinforced concrete wall elements were found to be conservative in calculating the ultimate loads of the specimens.

Chang (59) studied the effects of using fibreglas reinforcement on ferrocement panels under bending. He found that the cracking strength of the composite panels could be greatly increased in comparison to corresponding conventional ferrocement panels. The energy absorption characteristics could also be increased by as much as 100%. Load-deflection curves predicted by using the concepts of

moment-curvature relationships were quite similar to that of the experimental results. However, the ultimate deflections of the specimens predicted was much smaller than those obtained from test results.

Khan (60) studied the shear transfer between steel plate and concrete in flexure. Epoxy, shear studs and natural bond were used. A sand blasted steel surface plus epoxy provided adequate shear transfer, although shear studs allowed the greatest ductility. Ferrocement composite beams were found to be twice as strong but less ductile than reinforced concrete composite beams.

Preliminary ferrocement mixes in relation to compressive strength, volumetric stability and workability under a warm marine environment was investigated by Kowalaski (61). Shell effect in ferrocement vessels was studied by Torgeir Moan (62). A finite element analysis was carried out to find membrane and bending stresses in the shell. Simplified calculation procedures were proposed.

Chapter III

EXPERIMENTAL PROGRAM

3.1 Introduction

The behavior of ferrocement specimens subjected to combined tension and compression was studied by testing ten ferrocement elements of test section 7.9 inch. wide x 7.9 inch. long x 1.2 inch thick (200 mm. x 200 mm. x 30 mm.). The specimens were divided into three series depending on the specimen geometry and the steel content used. A special tension loading frame was designed to fit into a Baldwin Testing Machine so that tension and compression could be applied simultaneously. Tension force was transmitted to the test section through bolts embedded in the enlarged ends of each specimen. Compression force was applied directly to the test section. For each test, compression and tension loads, and corresponding compression and tension strains were recorded. The strains were measured by electrical resistance strain gauges as well as mechanical demec gauges. A general discussion of the experimental program is presented in the following sections.

3.2 Specimen Geometry

The specimens were cast in wood moulds. The shape and dimensions of the specimens are shown in Figure 3.1. The first three specimens were cast with enlarged ends in both vertical compression and horizontal tension directions. The other specimens were cast without enlarged ends in the vertical compression direction.

The cross-section of the test section was kept constant at 1.2 inches thick and 7.9 inches wide (30 mm. x 200 mm.). This size was chosen because it was neither too large to handle nor too small to obtain reliable results. The uniformity of the cross-section was maintained over a length of 10 inches (250 mm.). The cross-section was then gradually increased to 12 inches x 3.2 inches (300 mm. x 80 mm.) in the horizontal tension direction. The horizontal enlarged cross-section was maintained constant for 5.9 inches (150 mm.) at both ends. Four 5/8-inch diameter bolts were placed at each end. The distance between centres of two bolts was 2.95 inches (75 mm.) and the length of the bolts embedded in mortar was four inches (100 mm.). The thickness of the enlarged ends was increased to 3.2 inches so that spirals of two inches in diameter could be inserted around the bolts to act as shear and confinement reinforcement.

For specimens 1 to 3, the test sections were enlarged in both vertical and horizontal directions. The horizontal enlarged ends were the same as described above. In the vertical direction, the cross-section was first extended 1 inch (25 mm.) above and below the section with same thickness of 1.2 inches. The vertical ends were then gradually increased to 3.2 inches thick and 7.9 inches wide over a length of 1 inch (25 mm.). The thickness and width were then kept constant over a length of 1 inch. The length of the enlarged ends was 7.9 inches (200 mm.).

3.3 Materials Used

The mortar consisted of ASTM Type III, high-early strength, Portland cement and fine sand passing sieve No. 4. The water-cement

and sand-cement ratios by weight were 0.48 and 2.0 respectively for all specimens. The average cylinder compressive strength of mortar at the time of test was about 7300 psi (50.3 KN/m^2) and the average horizontal tensile strength from split cylinder tests was about 468 psi (3.2 KN/m^2).

Welded square galvanized mesh of size 1/2 inch x 1/2 inch (1.27 cm. x 1.27 cm.) was used as reinforcement. The properties of the wire mesh is shown in Table 3.1. The yield strength of the mesh was obtained by performing a tension test on 12 single wires from each test series and then taking the average yield strength.

Four ASTM A325 bolts of diameter 5/8 inches were embedded in each end of a specimen. Two-inch-diameter spirals made from number 9 gauge wire were placed around each bolt to confine the mortar. Hooks made of number 9 wire were used to keep the spirals in place and to provide shear strength. The detail of the reinforcement is shown in Figure 3.2.

3.4 Casting and Curing of Specimens

All specimens were cast in wood moulds. The wood mould was made of 3/4-inch plywood. Its inside dimensions were 27.6 in. x 11.8 in. x 3.2 in. (700 mm. x 300 mm. x 80 mm.). Wood blocks were fixed into the mould so as to get the required shape of the specimens. Four holes were drilled in each end block to let the 5/8-in.-diameter bolts pass through. The end blocks were two inches thick so that the bolts could be placed as straight as possible by resting the bolts in the holes. The holes, and therefore the bolts, could easily be controlled and kept in good alignment with those in the other end of the mould.

This was to ensure that no bending was induced when tension was applied to the bolts during testing. Since the specimen was enlarged in two directions, a top cover slightly shorter than the mould was made separately. The top cover was connected to the mould by using four 6-in. long bolts of diameter 5/8 inches.

In preparing the reinforcement, the wire mesh was first cut and bent into layers slightly smaller than the mould. Four spirals were placed in both enlarged ends with equal number of mesh layers above and below the spirals. Two hooks were placed around each spiral. The mesh layers were spread by a small strip spacer and tied together to form a block package of mesh. At the transition zones, extra wire mesh layers of 1 in. x 8 in. were used to provide more reinforcement against any stress concentration at corners. The package of mesh was then placed inside the wood mould. The 5/8-in. diameter bolts were placed through the holes of the end blocks and were embedded four inches inside the mould.

The required weight of sand, cement and water was measured. The materials were mixed in a standard mixer with rotating drum for about three minutes. The mortar was then cast into the mould and was vibrated on a vibrating table for about three minutes to obtain uniform compaction. The top cover of the mould was pressed and bolted down to squeeze out the excess mortar. The compacted specimen was then covered with a plastic sheet to prevent any loss of moisture. One specimen and four standard cylinders were prepared from each mix. The specimen and the cylinders were stripped 24 hours after casting and then cured in moist room for seven days. They were then left in the laboratory environment for a drying period of seven days before testing.

3.5 Specimen Instrumentation

In order to study the stress-strain behavior of ferrocement under combined tension and compression, local and average elongations of a test section were measured by concrete strain gauges and mechanical demec gauges respectively.

Two strain gauges, one longitudinal and one lateral, were mounted on the centre of each specimen. Type SR-4 electrical resistance concrete strain gauges of length 1.5 inches were used. Their gauge factor was 2.095. The recorded readings from the strain indicator were used to determine the stress-strain relationships and Poisson's Ratio of ferrocement under biaxial loading. On the other side of the specimen, mechanical demec gauges were mounted in both longitudinal and lateral directions. The distance between the demec gauges in each direction was five inches in the first two specimens and two inches in the others. The positions of the electrical strain gauges and the mechanical demec gauges are shown in Figure 3.1.

Steel strain gauges were mounted on the four 5/8-in. diameter bolts in the tensile loading end with one gauge on each bolt. They were connected to a strain indicator so that the tensile strains induced on each bolt could be measured and adjusted to give equal amount of strain in the four bolts during loading. This was to eliminate or minimize the effect of bending that would have been induced if the strains. and therefore stresses. in the four bolts were different.

The applied tension load from a 30 ton capacity hydraulic jack was measured by using an electrical-resistance strain-gauge load cell. The load cell was calibrated before the test series on the

Baldwin Testing Machine. The relationship between the applied tension loads and the strain indicator readings was linear with an increase of 10 kips for every strain increase of 500 micro-inches per inch.

3.6 Test Equipment and Procedure

The investigation was carried out in the Civil Engineering Laboratory at the University of Alberta. Specimens were loaded in compression by using a 200,000 lb. capacity Baldwin Testing Machine. A special frame for tension loading was designed so that it could be fitted on the lower compression platten of the Baldwin Testing Machine. A 30 ton capacity centre hole hydraulic jack was used to apply tension to the specimens. Loading exerted by this jack was measured by a 50-ton capacity load cell which was calibrated before the test series. For each test, tension was held constant at a designated value while compression was increased until failure occurred.

3.6.1 Test Set-up

The test set-up was as shown in Figure 3.3. Compression was applied to the test sections by moving the lower platten of the Baldwin Testing Machine upward. Steel blocks of cross-section 3.5 in. x 2 in. x 8 in. (89 mm. x 51 mm. x 203 mm.) were used to transmit the compressive force to the test sections. Since the ends of the specimens 4 to 10 were not enlarged in the vertical compression directions, extra steel blocks of cross-section 1.2 in. x 2-7/8 in. x 6 in. (30 mm. x 75 mm. x 152 mm.) were inserted at top and bottom of the specimens. During each test, the specimen and the steel blocks were centrally and vertically placed on the bottom compression platten of the Baldwin

Testing Machine. Two strips of 1/4-in. plywood were placed between the specimen and the steel blocks so as to eliminate the end restraints on the specimen.

The tension loading frame consisted of four 2-in. diameter bolts and two 2-in. thick steel plates. The steel plate held the bolts in place and provided supports on the reaction exerted from the hydraulic jack when tension was applied. The tension loading frame was placed on two rollers. The rollers were two inches in diameter and were placed on the lower compression platten. Since the lower compression platten moved up during compression loading, the whole tensile testing frame moved up as well. Therefore the tension frame could follow small movements of the specimens in both directions without generating appreciable secondary stresses in the specimens. Tension was transmitted from the hydraulic jack to the specimen through a steel bracket to which the 5/8-in. diameter bolts were attached. Each steel bracket (Figures 3.4,3.5) consisted of a 3/4-in. steel base plate with four 11/16-in. diameter holes, two 3/8-in. side plates welded to the base plate and a steel rod of 1-in. in diameter. The steel rod was pin-connected to the side plates and passed through the 2-in. thick steel plate. On the loading end, the steel rod was extended to allow room for clamping the hydraulic jack and the load cell to the tensile loading frame. The 30-ton capacity centre hole hydraulic jack was connected between the tensile testing frame and the 50 ton capacity load cell. The load cell was connected to a strain indicated which was calibrated to measure the applied tension.

3.62 Test Procedure

After a drying period of seven days in the laboratory, concrete strain gauges and mechanical demec gauges were mounted on the specimens. Steel strain gauges were mounted on the 5/8-in. diameter bolts in the tensile loading end only. During testing, an initial small amount of compression (half kip), was applied to keep the specimen and the tension loading frame in proper position. Then a small tension force was applied. The degree of tightness of the nuts on the 5/8-in. bolts were checked and adjusted by making the strains in the four bolts approximately equal. This was to eliminate any bending that might have been induced on the specimen. For each specimen, the tension load was applied to its designated test value. The tension was then held constant while compression was increased in increments of 10 kips until failure occurred. Readings from the strain gauge indicator and the mechanical demec gauges were recorded for each increment of loading. On completion of the test, photographic records were made to show the cracking patterns.

Test Series	Specimen Numbers	Mesh Size (in. x in.)	Wire Diameter (in.)	Number of Layers	Yield Strength (ksi)	Percent of Longitudinal Volume of Reinforcement	Specific Surface (in^{-1})
1	1 - 3	½ x ½	0.050	6	65	2.0	3.14
2	4 - 6	½ x ½	0.050	6	65	2.0	3.14
3	7 - 10	½ x ½	0.042	10	65	2.4	4.40

Table 3.1

Properties of wire mesh reinforcement

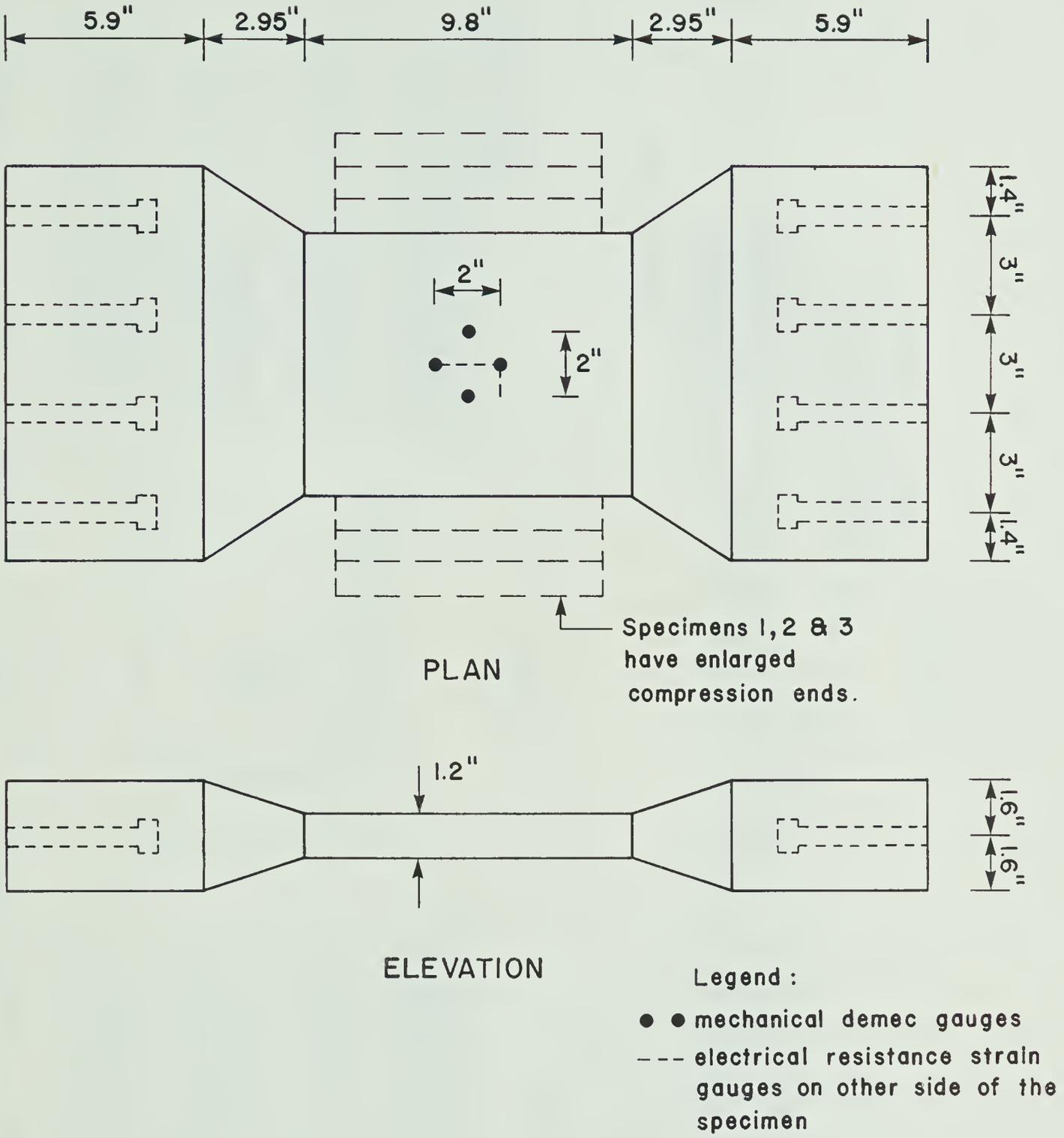

Fig. 3.1 Shape and Dimensions of
Test Specimens

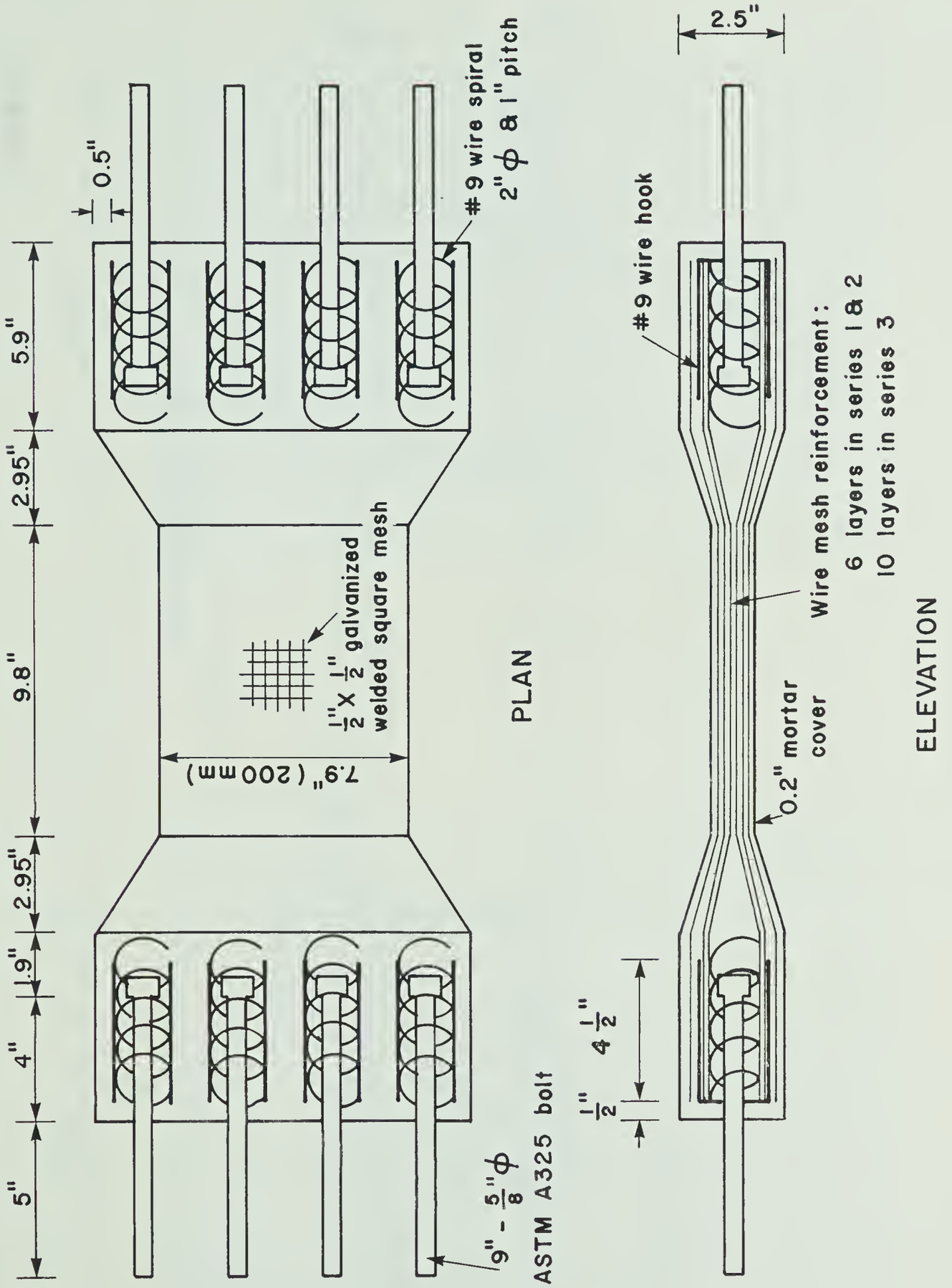

Fig. 3.2 Reinforcement Detail

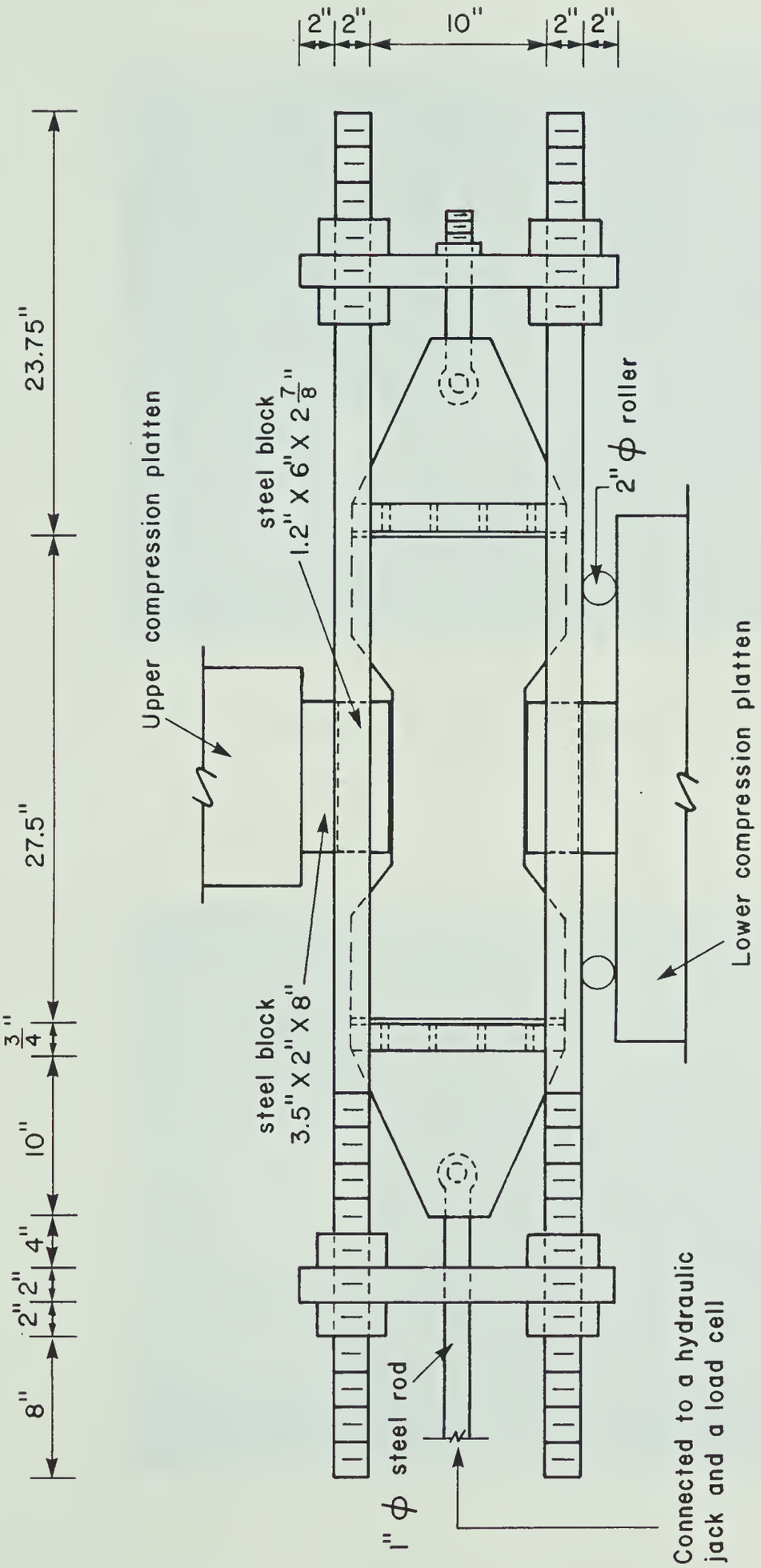

Fig. 3.3 Test Set-up

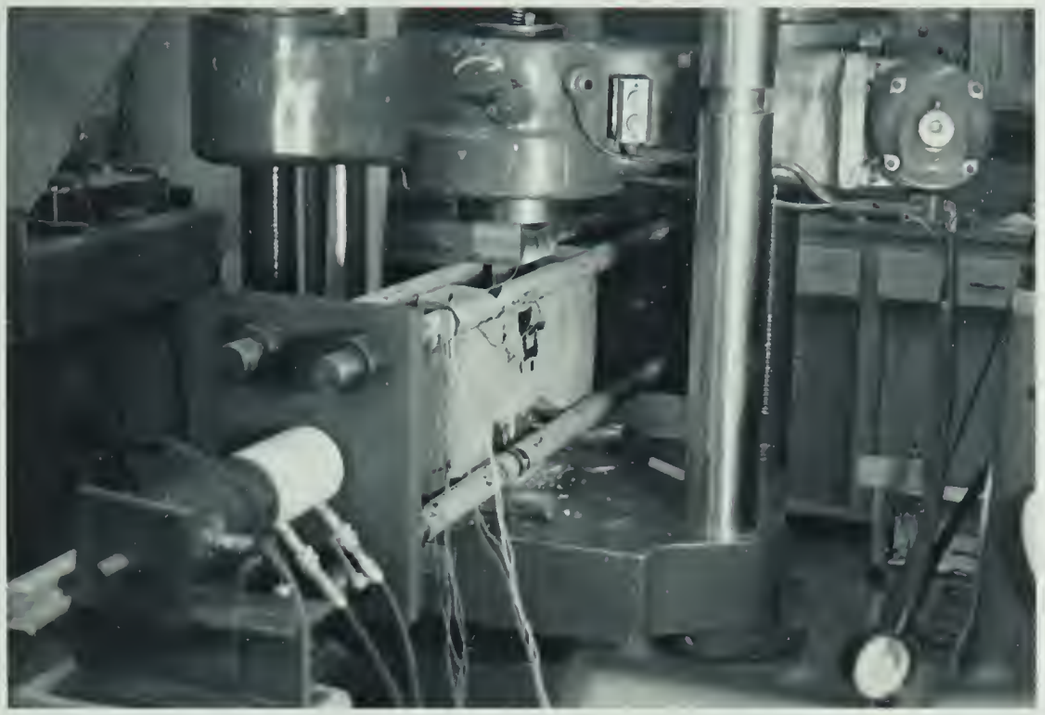

Figure 3.4 Tensile Loading Frame

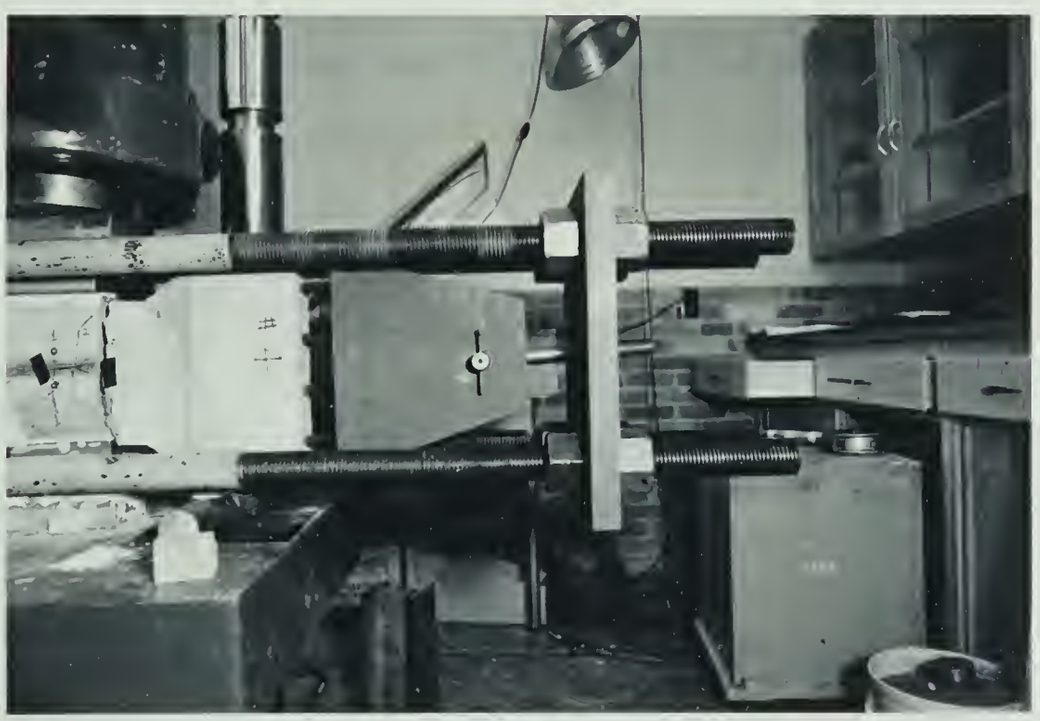

Figure 3.5 Steel Bracket

Chapter IV

TEST RESULTS

4.1 Introduction

The test results of the ten specimens are presented in this chapter. All the specimens were tested to failure by applying seven to eight increments of compressive load at a constant designated tensile load. The results were obtained directly, or calculated from readings during testing. The measurements taken were those of the electrical resistance strain gauges, the mechanical demec gauges, the calibrated load cell, and the Baldwin Testing Machine following each increment. The principal test results are summarized in a tabular manner. The graphical results include the load-strain relationships for the specimens derived from the strain gauge readings. The photographs were taken after each specimen failed. They show the cracking and failure patterns of the specimens tested.

4.2 Summary of Test Results

Table 4.1 gives a summary of the principal test results including failure loads and corresponding stresses, the splitting and compression strengths of the mortar, and the calculated moduli of elasticity and Poisson's ratios. For each specimen, the tension load was held constant at its designated test value. Therefore the failure load corresponds to the maximum compression load, C_{max} carried by the specimen. The modulus of elasticity of each specimen is the

secant modulus through 0.5 C_{max}. The values are compared with the theoretical modulus of elasticity of mortar calculated according to section 8.3.1 of ACI-318-71 by assuming that the mortar is normal weight concrete. The Poisson's ratios are calculated by using the generalized Hooke's Law in the plane stress condition. This will be discussed in the next chapter. The reinforcement details are not included in the table but are given in Chapter 3.

4.3 Load-Strain Relationships

The load strain curves of the specimens are plotted in Figures 4.1 to 4.12. The strains are those read directly from the electrical resistance strain gauges. Strains in both tension and compression directions are plotted. The load strain relationships of the specimens under combined tension and compression are plotted in figures 4.1 to 4.10 in numerical order of the specimens tested. Specimens 1 and 2 were tested in pure compression after they failed in the transition zone under combined tension and compression. The compression-strain curves obtained are plotted in figures 4.11 and 4.12.

4.4 Illustrative Cracking and Failure Patterns

Photographic plates showing typical cracking and failure patterns of some specimens tested are presented in figures 4.13 to 4.16.

Specimen	Failure Load		Failure Stress		f'_c (psi)	f_{sp} (psi)	Modulus of Elasticity of Mortar (ACI Eqn.) ($\times 10^6$ psi)	Modulus of Elasticity of Mortar from Test ($\times 10^6$ psi)	Modulus of Elasticity of Ferrocement ($\times 10^6$ psi)
	Tension (kips)	Comp. (kips)	Tension (psi)	Comp. (psi)					
1	10.8	45	1125	4688	7050	464	4.8	3.2	4.6
2	8	18	833	1875	6793	500	4.7	3.2	-
3	4	80.7	417	8406	6349	411	4.5	3.0	4.4
4	6	55	625	7639	7270	411	4.9	3.4	4.4
5	4	54	417	7500	8250	495	5.2	3.4	3.1
6	8	59.4	833	8250	7550	470	5.0	3.2	4.9
7	4	63	417	8750	8913	524	5.4	3.3	5.1
8	2	54	208	7500	6767	469	4.7	2.7	4.1
9	6	53	625	7361	7393	455	4.9	3.0	4.2
10	8	55	833	7639	6765	480	4.7	2.8	4.2

Table 4.1

Summary of Test Results

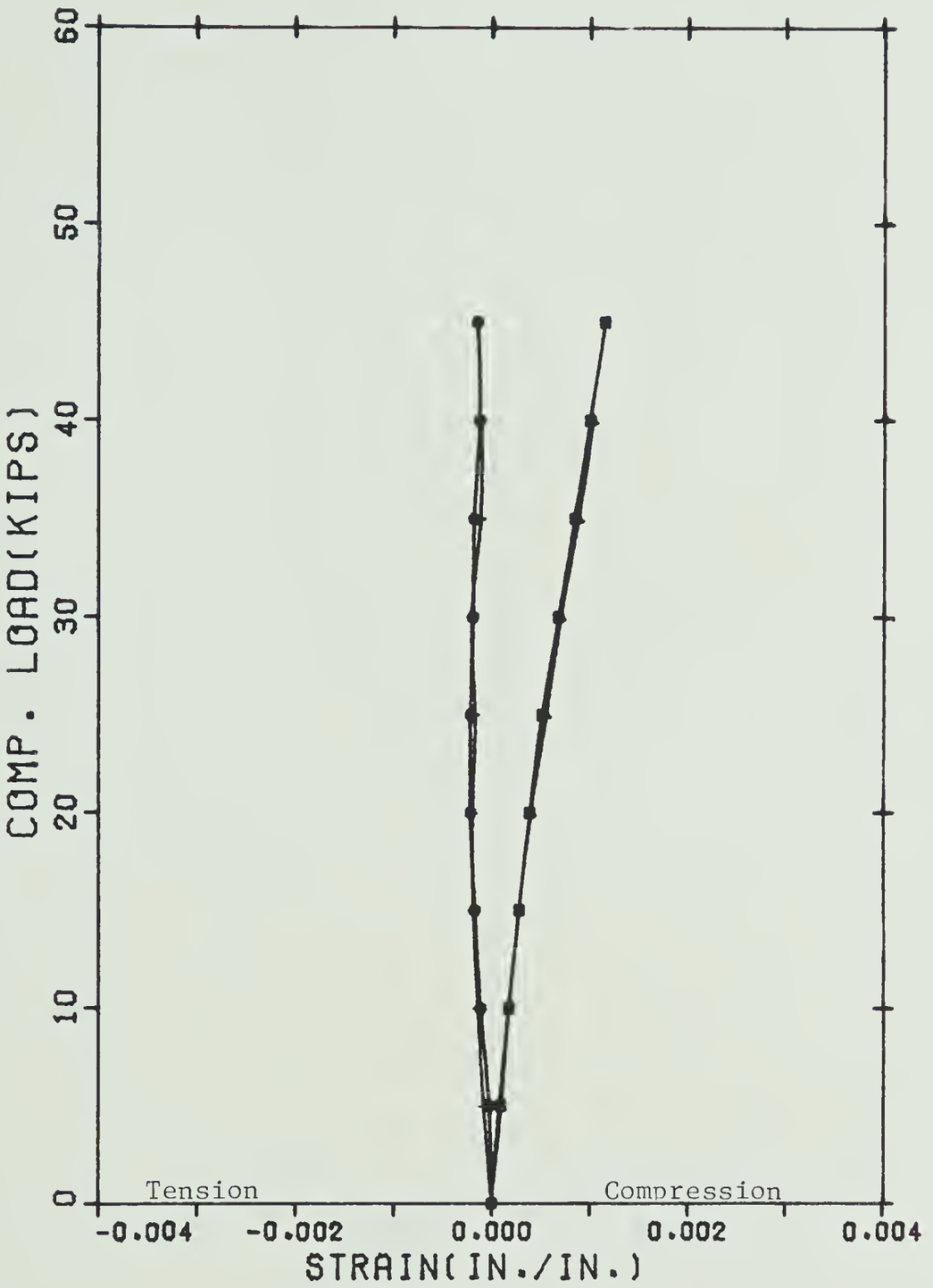

Figure 4.1

Load vs Strain for Specimen 1

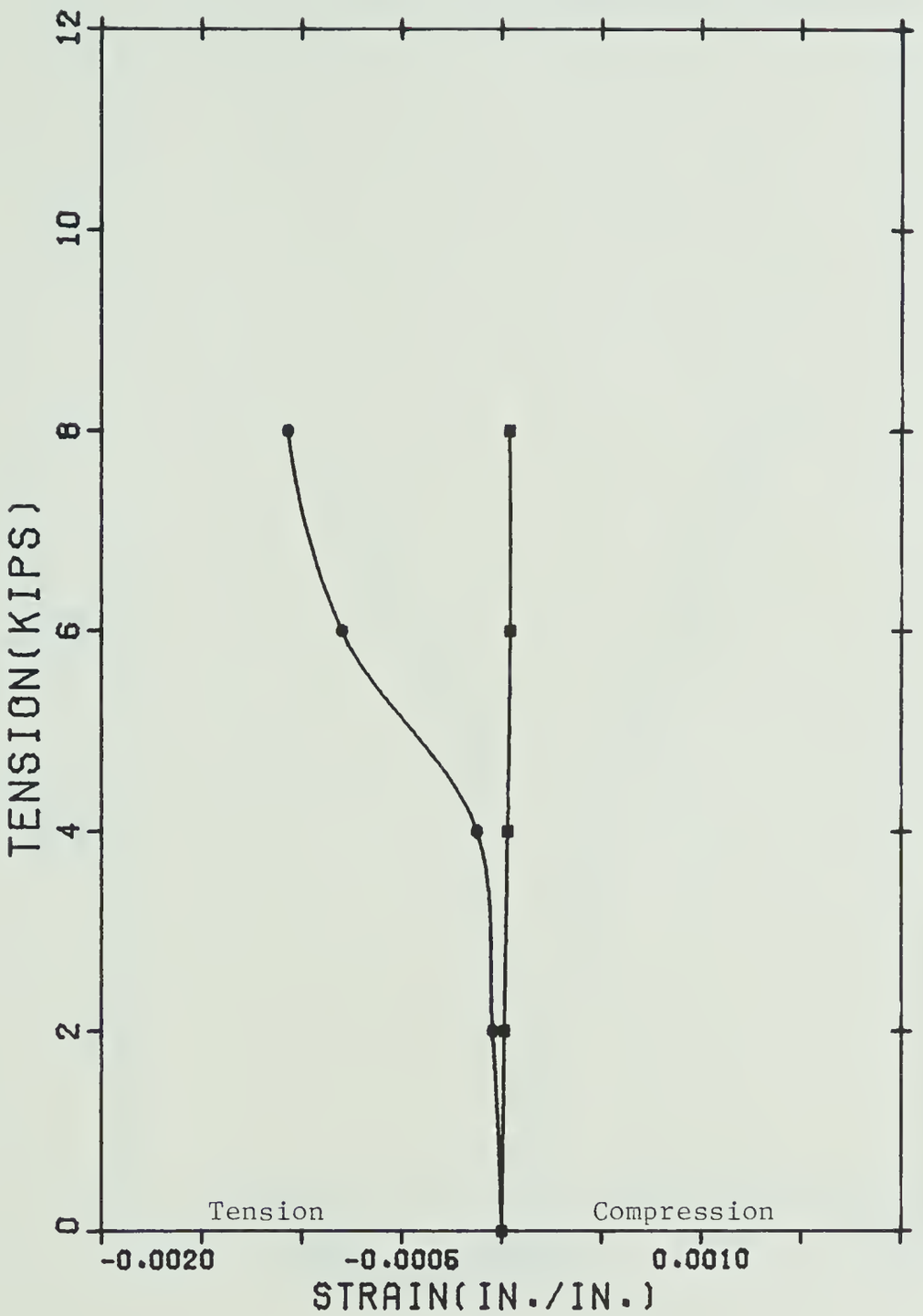

Figure 4.2

Load vs Strain for Specimen 2

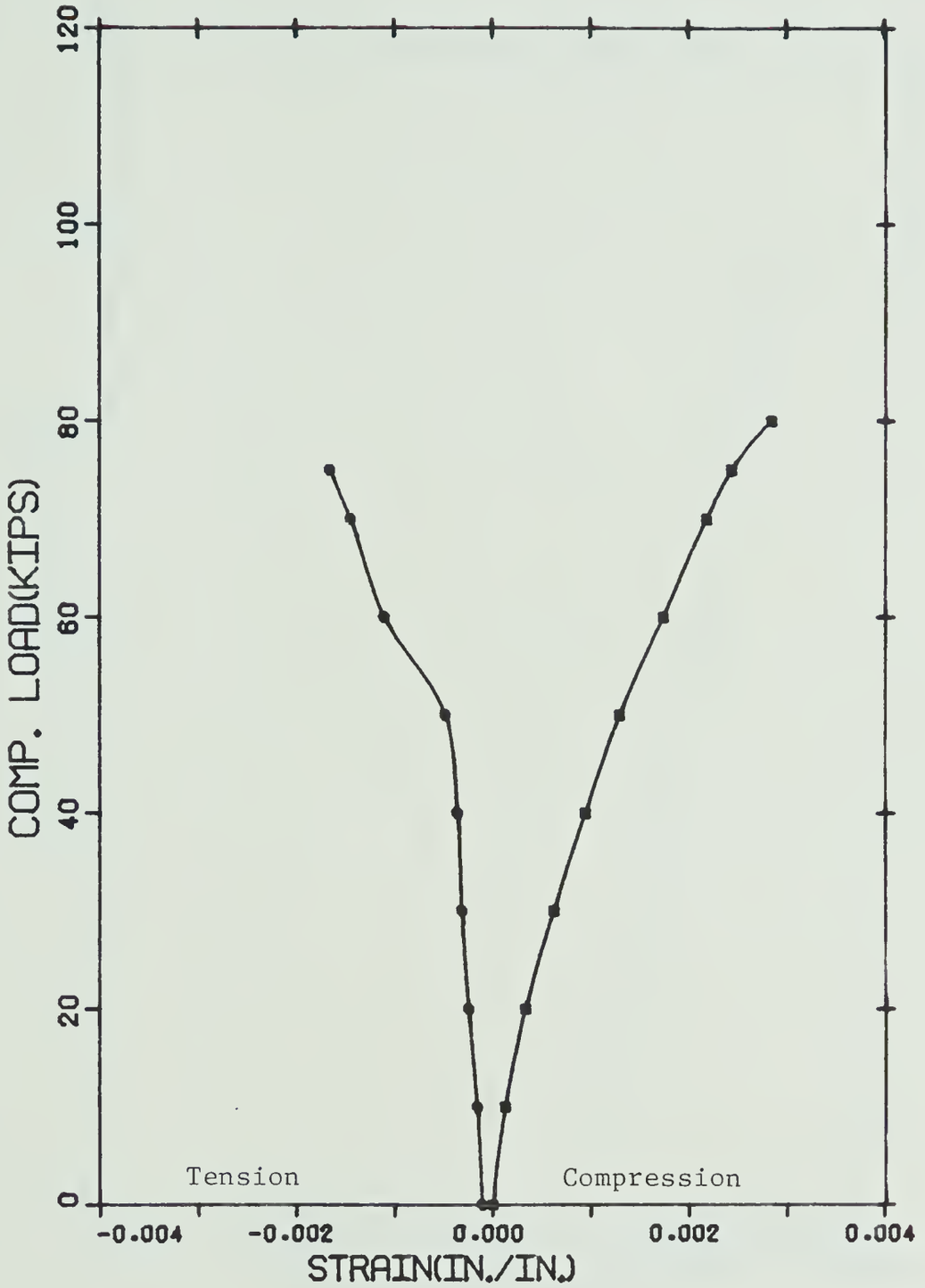

Figure 4.3

Load vs Strain for Specimen 3

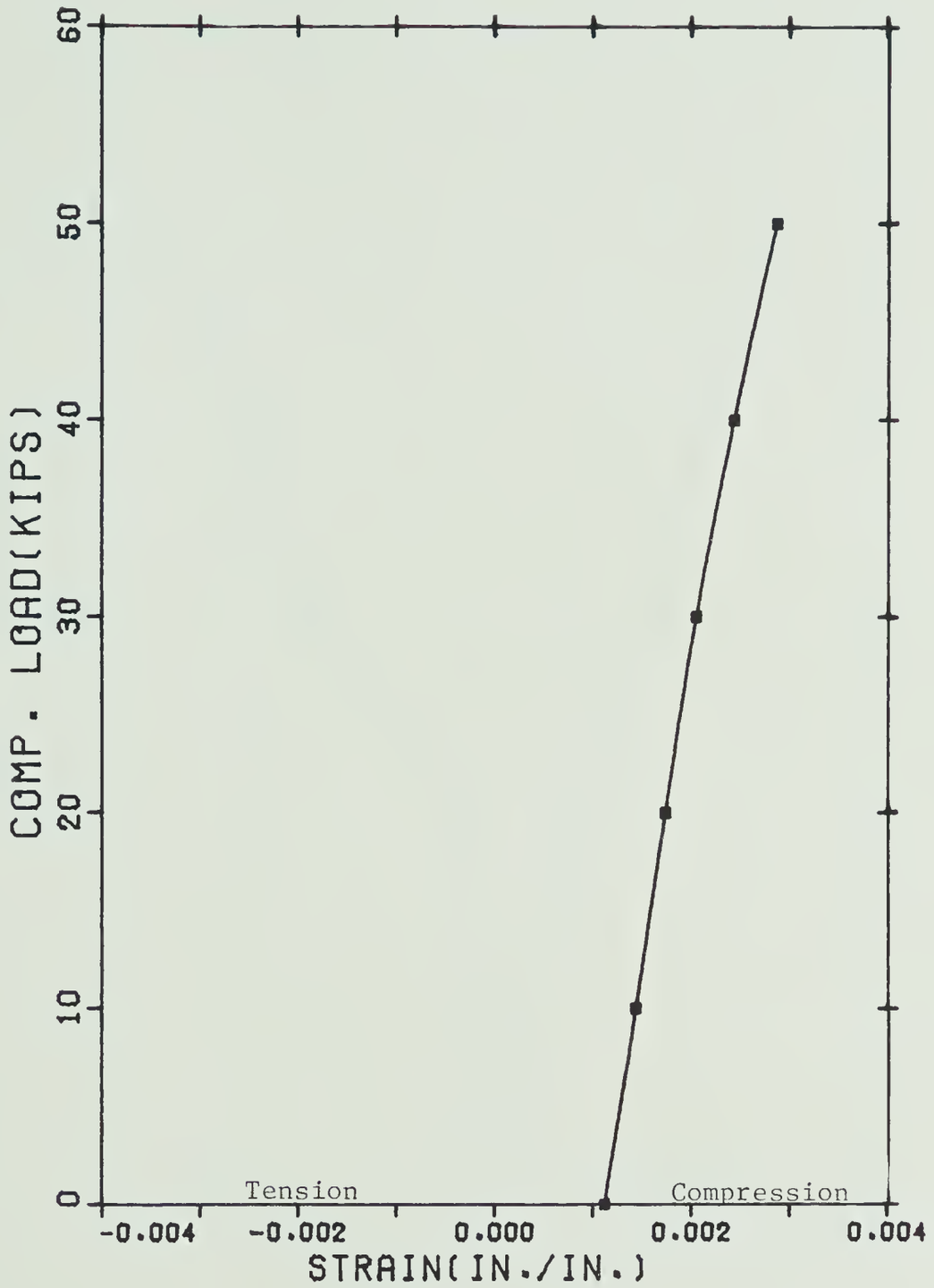

Figure 4.4

Load vs Strain for Specimen 4

Figure 4.5

Load vs Strain for Specimen 5

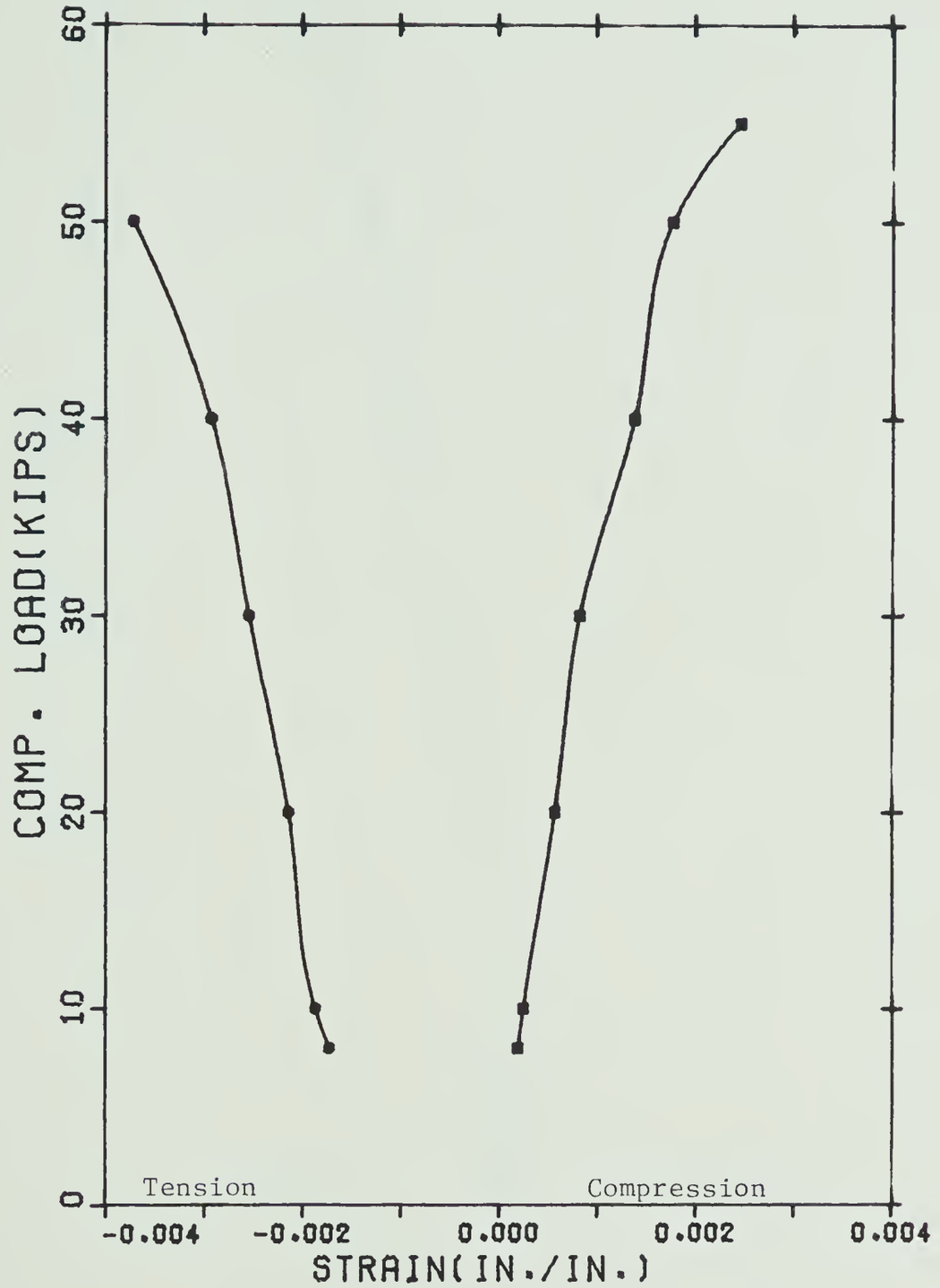

Figure 4.6

Load vs Strain for Specimen 6

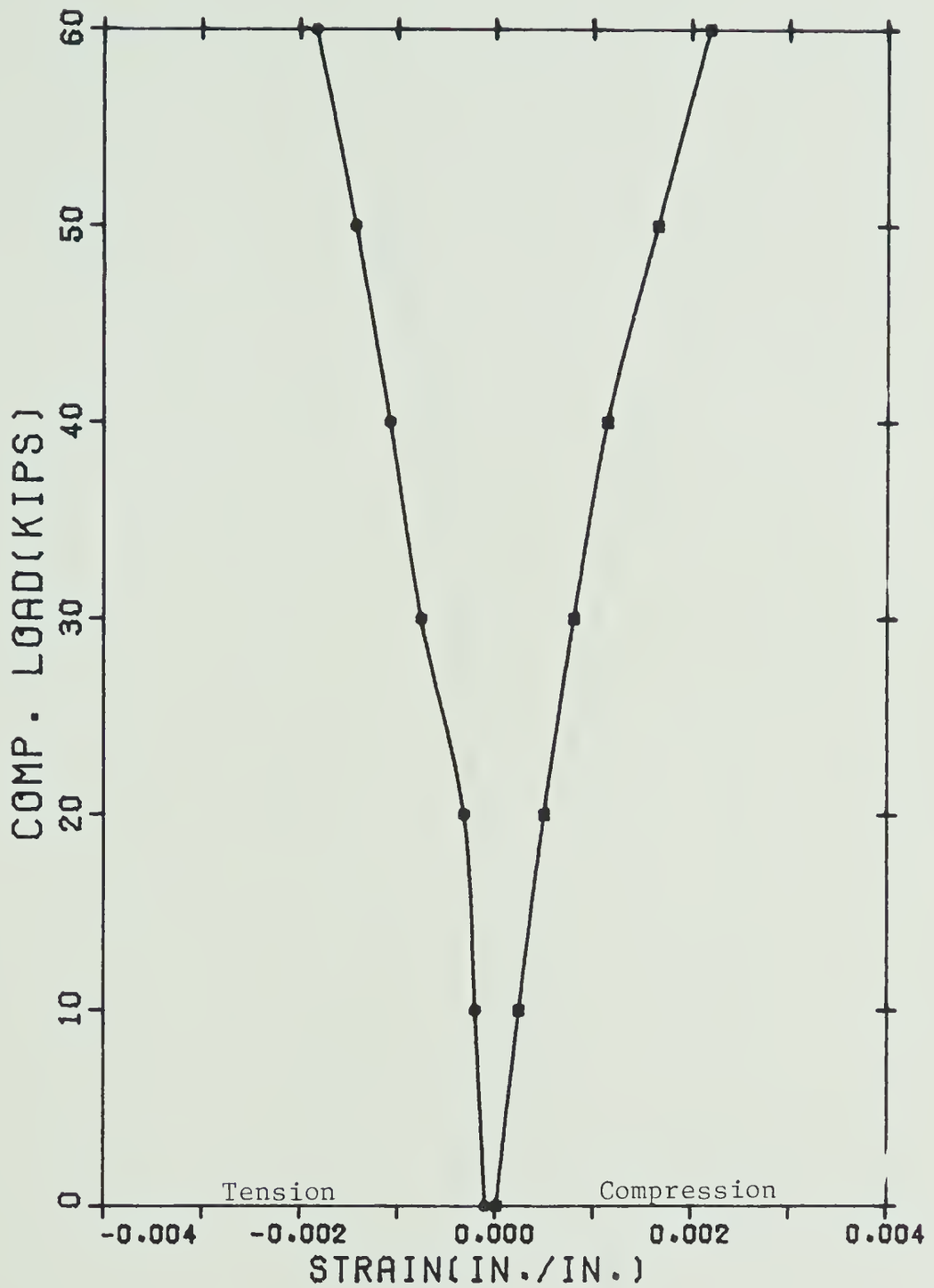

Figure 4.7

Load vs Strain for Specimen 7

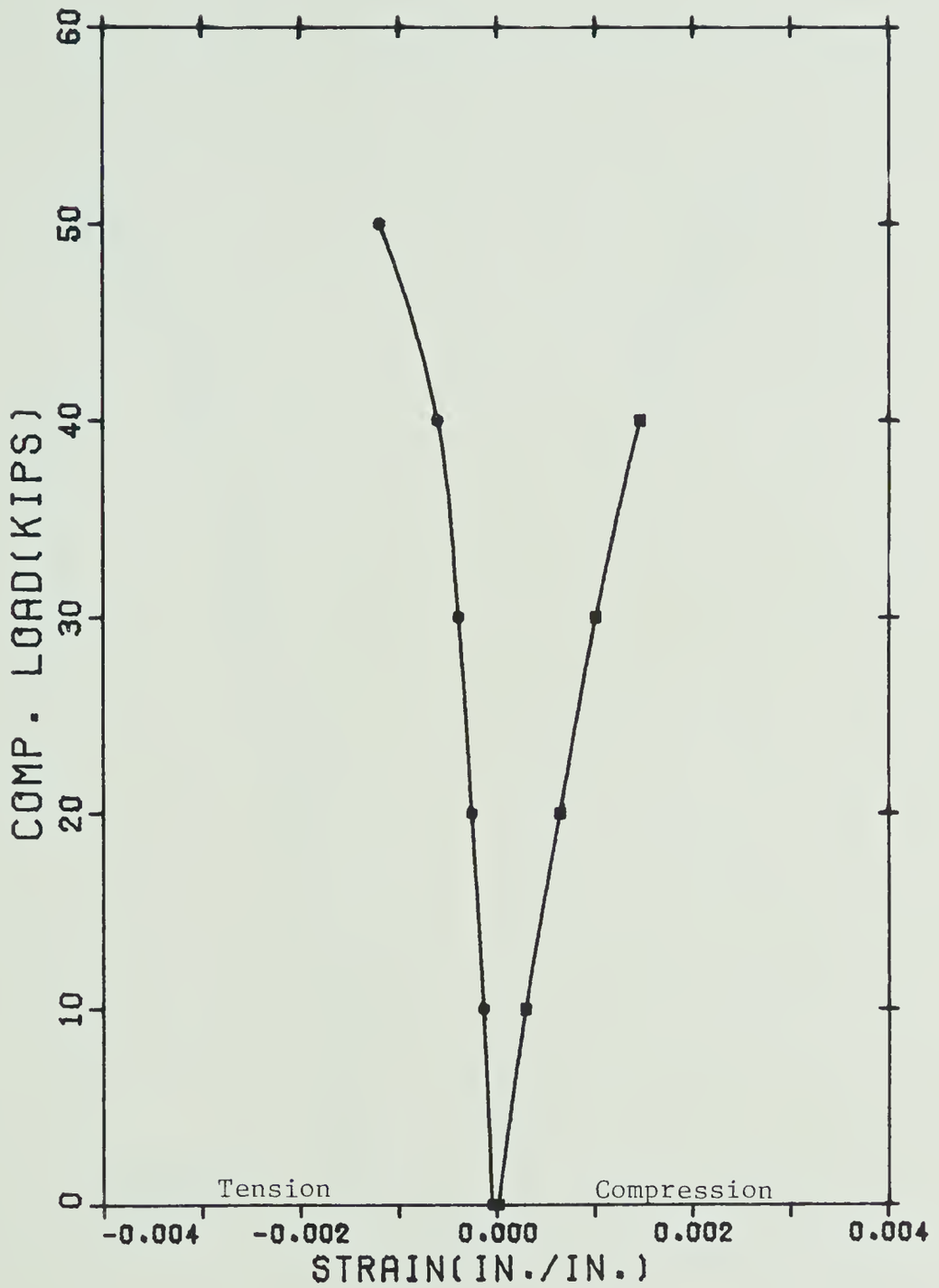

Figure 4.8

Load vs Strain for Specimen 8

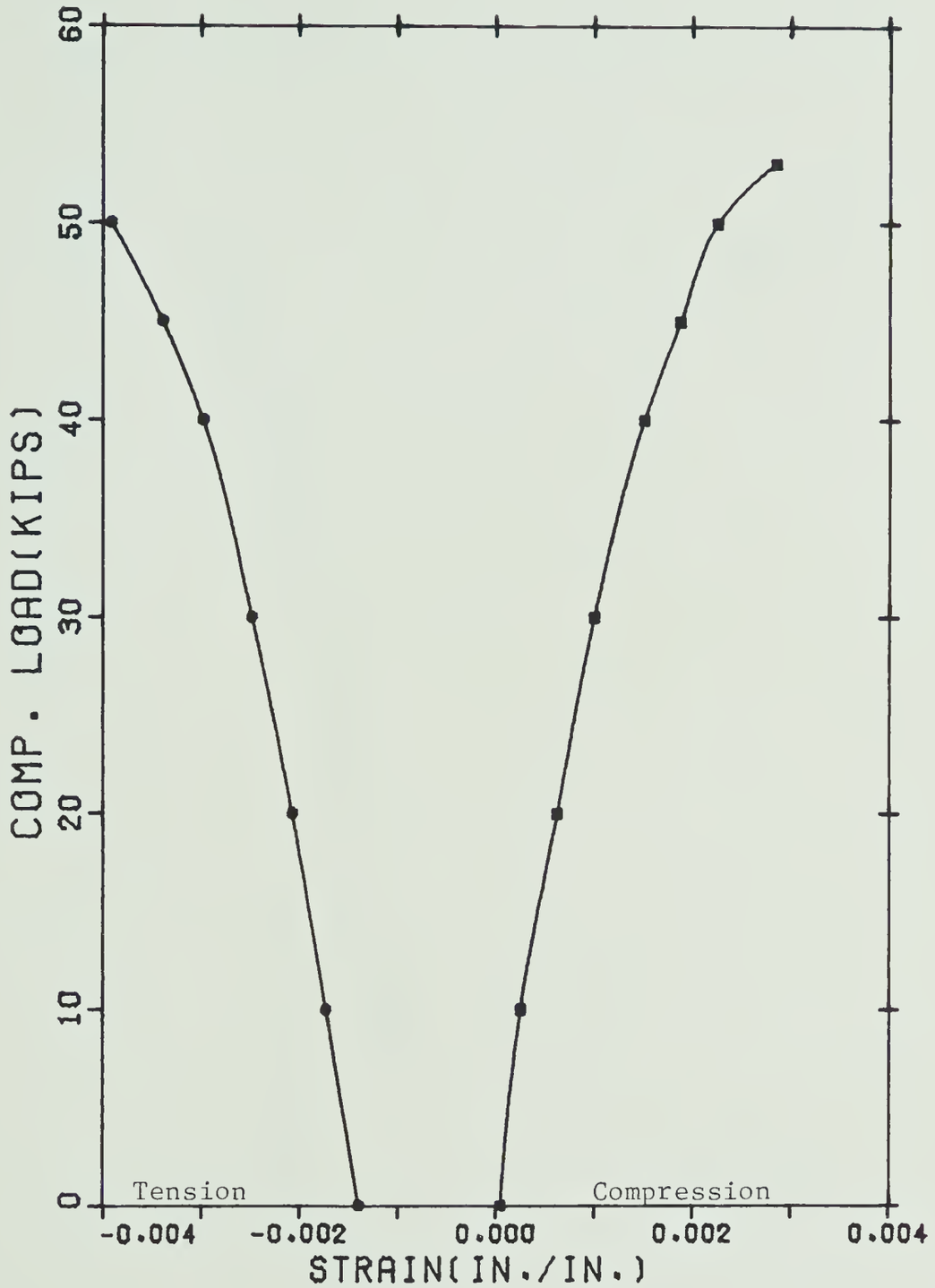

Figure 4.9

Load vs Strain for Specimen 9

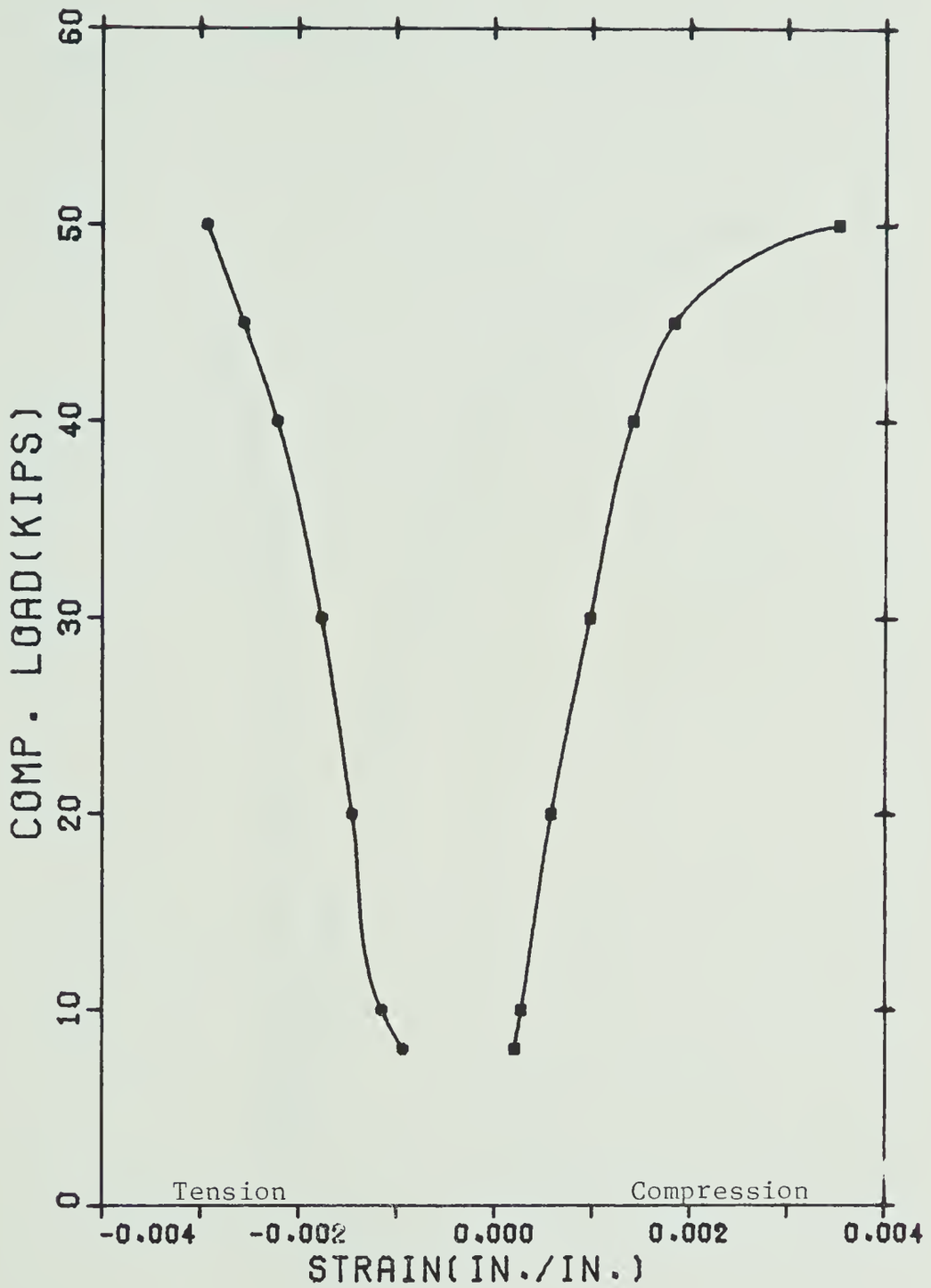

Figure 4.10

Load vs Strain for Specimen 10

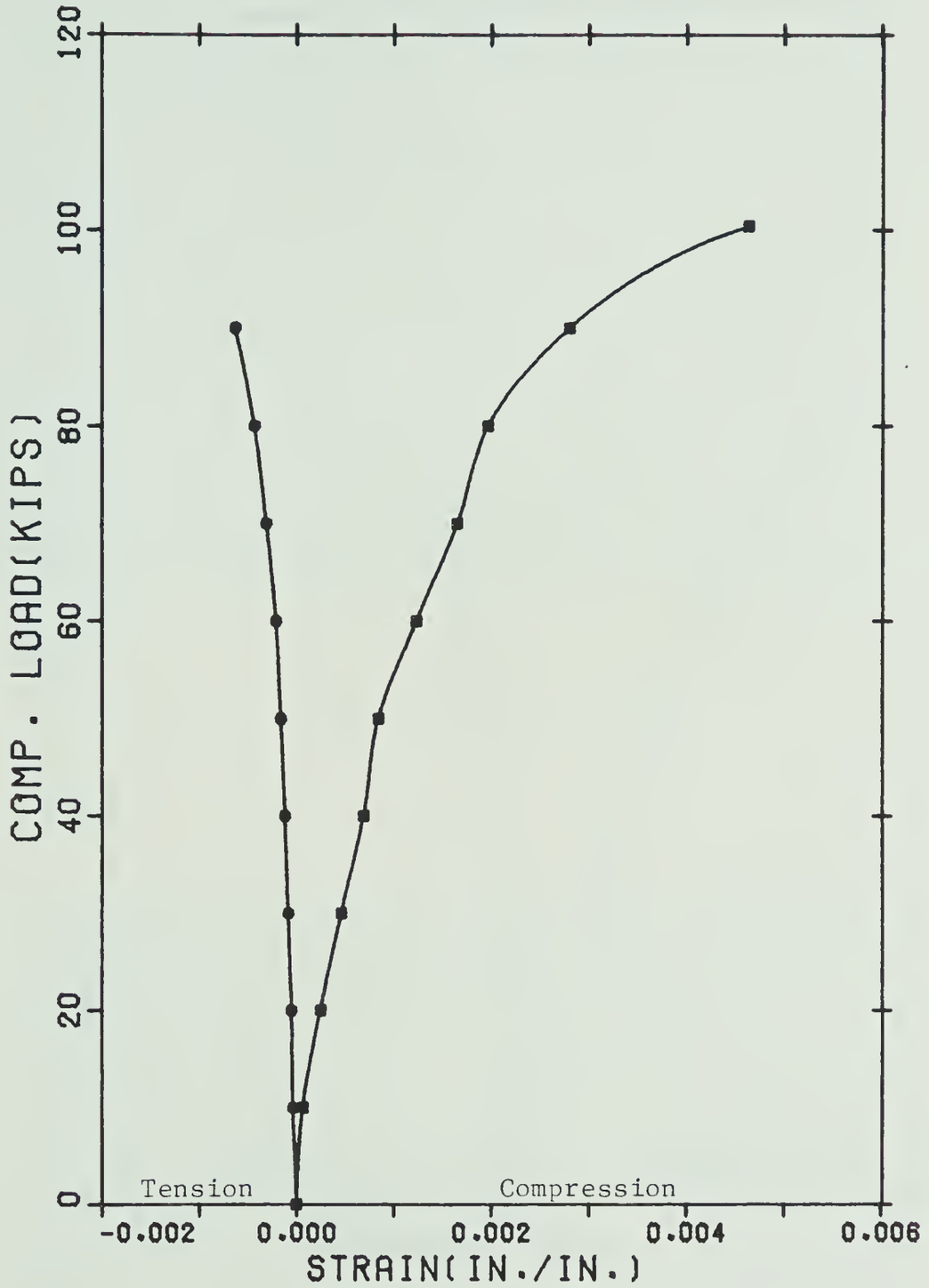

Figure 4.11

Load vs Strain for Specimen 1 after Failure

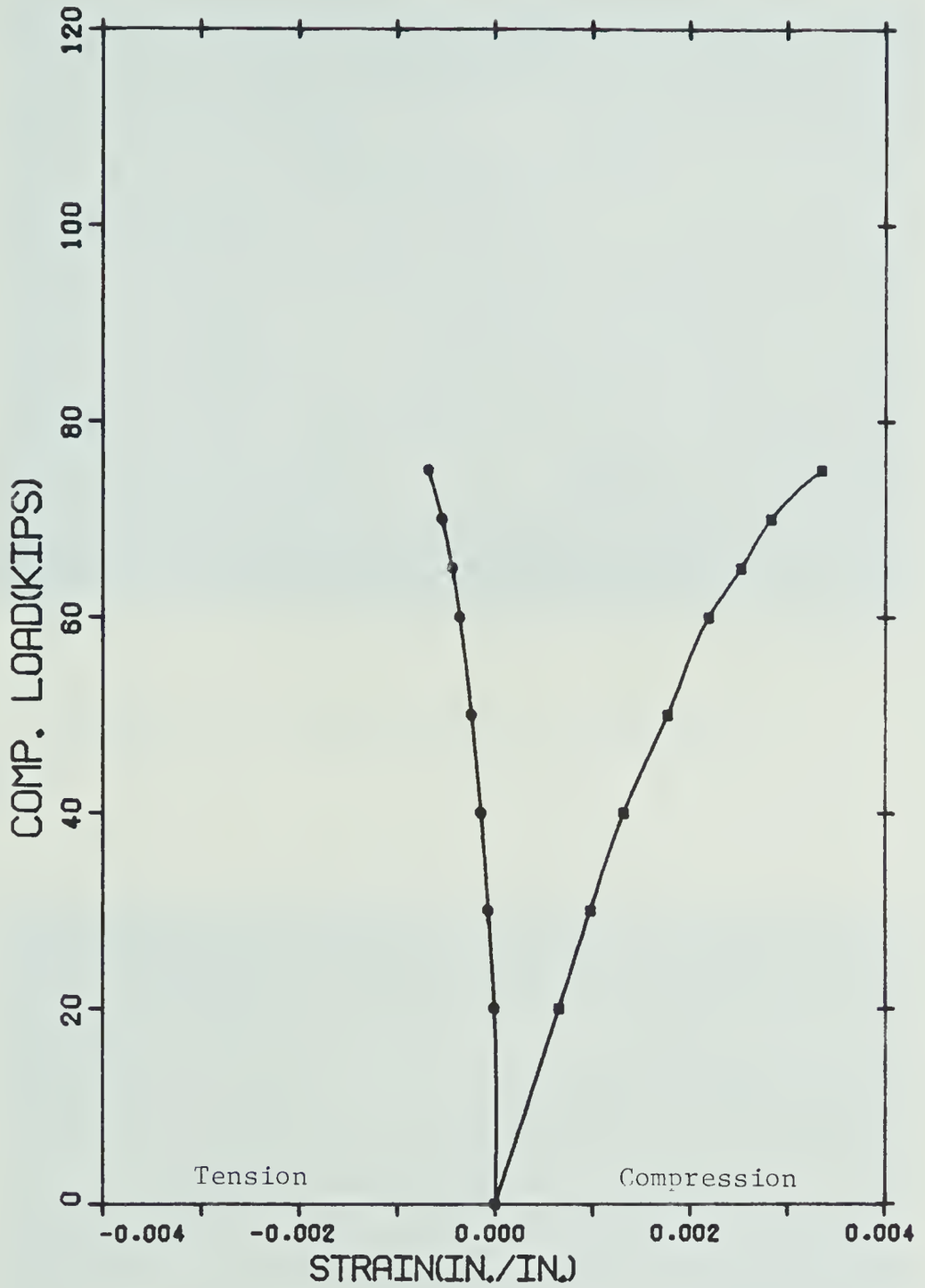

Figure 4.12

Load vs Strain for Specimen 2 after Failure

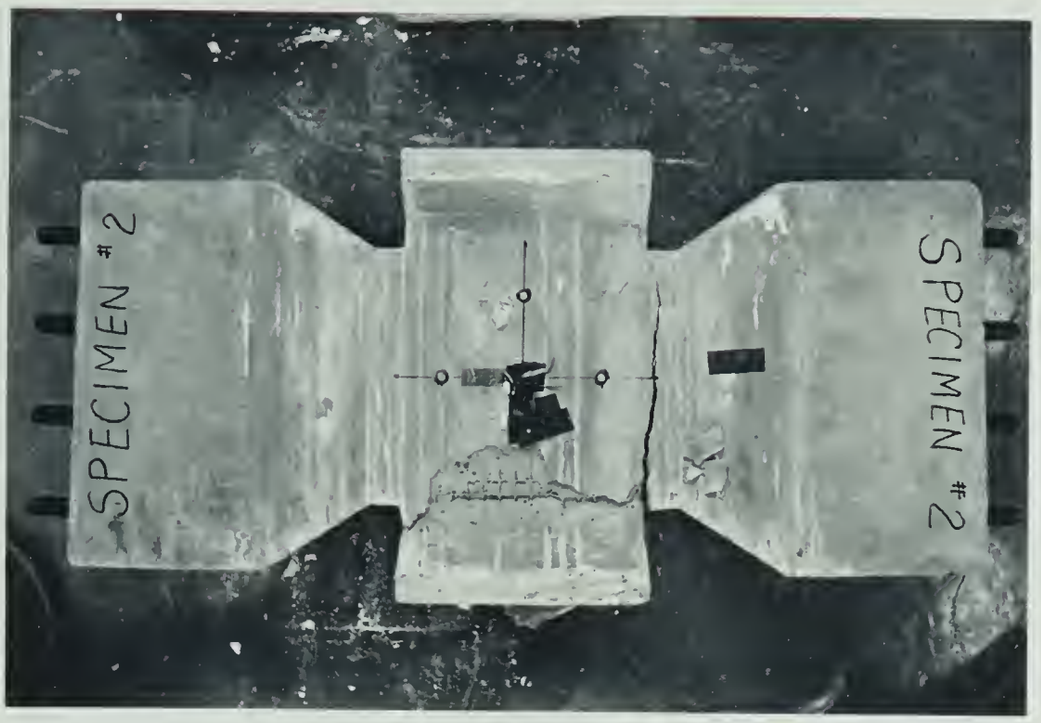

Figure 4.13 Failure Pattern of Specimen 2

Figure 4.14 Failure Pattern of Specimen 6

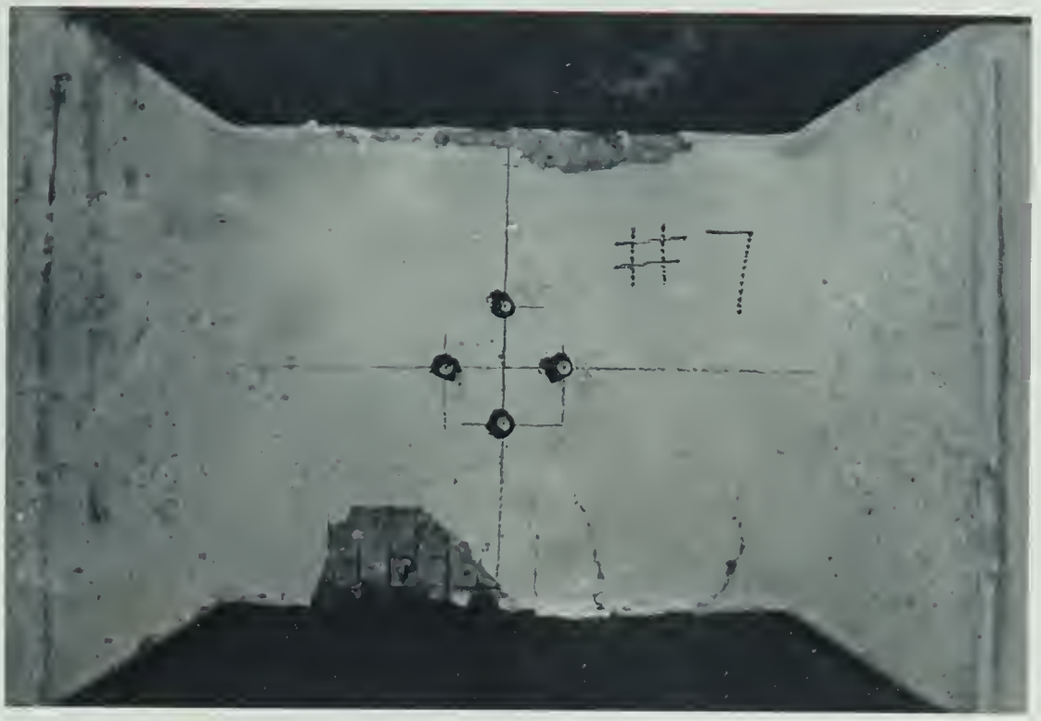

Figure 4.15 Failure Pattern of Specimen 7

Figure 4.16 Failure Pattern of Specimen 10

Chapter V

DISCUSSION OF TEST RESULTS

5.1 Introduction

This chapter presents a discussion of the ten specimens tested under combined biaxial tension-compression and the effects of the major variables involved. The major variables were specimen geometry and amount of wire mesh reinforcement. The following discussion, supplemented by the figures in Chapter IV, describes the behavior of individual specimen in relation to the above variables and the applied designated tensile load. From the test results obtained, it appears that, under biaxial tension-compression, there was no significant interaction between the ultimate compressive strength of ferrocement and the applied tension for the range of loading used. The secant modulus of elasticity at 0.5 ultimate compressive strength and Poisson's ratio calculated from the test results are also discussed.

5.2 Behavior of Test Specimens

The test program was divided into three series depending on the specimen geometry and the amount of wire mesh reinforcement. The load-strain curves of the specimens under biaxial tension-compression have been presented in Figures 4.1 to 4.12. During each test, no visible crack was observed until near failure of the specimen. The typical failure patterns of the specimens have been presented in Figures 4.13 to 4.16. The behavior of individual specimens is discussed in this section.

5.2.1 Series I

The specimens of this series differed with those of the other two series in that they have a different shape. The compression ends were enlarged. The amount of reinforcement used was equal to that in series II, but was less than that used in series III. The maximum uniaxial tension and compression expected were 12 kips and 65 kips, respectively. This was calculated on the basis that the tensile strength of the specimens depended on that of the wire mesh while the compressive strength of the specimens depended on that of the cement mortar.

Specimen 1 was loaded at a compression-tension ratio of 10/2.4. Compression increment was first applied and tension was then increased to the designated value. The specimen broke suddenly right across the transition zone at about 90 degrees with the tension loading direction when tension was increased to 10.8 kips at a compression of 45 kips. There was no visible crack or damage in the test section. Figure 4.1 shows the relationship of compression and tension strains with compression before and after the tension increment was applied. The curves are fairly linear up to the compression loading of 20 kips, which is about 0.45 of the maximum compression. In this range, at a given compression, there was no significant difference in compression strains before and after tension increment was applied.

Specimen 2 was first loaded only in uniaxial tension up to 8 kips. Figure 4.2 shows the tension-strain relationship. The compression strains are very small and increase fairly linearly with tension. There is a sharp increase in strain when tension is increased

from 4 kips to 6 kips. This may be due to the development of some micro-cracks in the mortar. When compression was increased to 18 kips at a tension of 8 kips, the specimen broke at the transition zone similar to specimen 1.

From the tension-strain curve of specimen 2, it was noted that the tension strain increased sharply when tension was beyond 4 kips. Therefore specimen 3 was loaded in compression at a constant tension of 4 kips. Figure 4.3 shows that the compression-tension strain is fairly linear up to a compression of 50 kips. At a compression of 30 kips, a crack initiating from the lower left hand corner was observed. The crack propagated to the centre of the test section. The specimen finally failed by the crushing of mortar. The maximum compression was 80.7 kips. This generated a compressive stress of 8400 psi on the test section. This stress was about 30 percent higher than the average compressive strength of the cylinders, which is 6350 psi.

The undamaged test sections of specimens 1 and 2 were tested in uniaxial compression after the specimens had failed in the transition zone under combined tension-compression. The load strain curves have been shown in Figures 4.11 and 4.12. Both specimens failed by crushing of the mortar. The maximum compressive load reached for specimens 1 and 2 were 100.4 kips and 78.4 kips, respectively. The corresponding compressive stresses generated were 10,460 psi and 8170 psi, which were higher than the cylinder compressive strength. The increase in compressive strength may be due to the following reasons:

(1) the wire mesh reinforcement provided lateral confinement to the mortar,

(2) the enlarged compression ends might contribute some compressive strength to the test section.

A typical cracking pattern of the three specimens is shown in Figure 4.13. This photograph was taken after specimen 2 was tested in pure uniaxial compression. Although specimen 3 was subjected to a tension of 4 kips as well as compression, its failure pattern was essentially the same as specimen 1 and 2 under uniaxial compression. They all failed by the crushing of mortar at the bottom of the test section.

In these specimens, the wire mesh reinforcements were extended to the enlarged compression ends. This extra reinforcement might have provided more tensile strength to the test section. The enlarged compression ends might also have provided restraint of horizontal movements of the test section when tension was applied. This restraint together with some stress concentration that might have arisen in the transition zone may be the reason why specimens 1 and 2 failed in the transition zones under combined tension-compression. The tension load applied to specimen 3 was relatively smaller, so that tension failure did not occur. From the test results, it seemed that, for biaxial tension-compression, it is better to apply compression directly to the test section than to transfer compression through enlarged ends.

5.2.2 Series II

This series consisted of three specimens which were similar to those in series I except that there were no enlarged compression ends in these specimens. The typical cracking pattern was shown in

Figure 4.14. During testing, visible tension cracks developed when compression was increased to about 50, 40 and 50 kips for specimens 4, 5 and 6, respectively. All three specimens failed by crushing of the mortar at the bottom.

One side of specimen 4 was found to have a small shrinkage crack after a curing period of 7 days. The crack extended from the top right hand corner of the test section to the centre. During testing, the horizontal tension strain gauge yielded at a very low applied tension of 2 kips. Therefore only compression strains were recorded and plotted against the compression loading as shown in Figure 4.4. Tension was kept constant at 4 kips and the ultimate compression load reached was 55 kips. The compression load-strain curve was linear up to about 30 kips which was about 50% of the maximum compression. At about 50 kips, tension cracks developed. On further increasing of loading, the wire mesh reinforcement at the bottom bulged out and mortar was crushed.

Figure 4.5 shows the compression load-strain curve of specimen 5. The specimen was loaded in compression to 54 kips at a constant tension of 4 kips. At 40 kips compression, a crack developed from the bottom.

From the load-strain curve, it can be observed that there was a sharp increase in tension strain when compression was increased from 20 kips to 30 kips while compression strains remained fairly linear with compression loading. The sharp increase in tension strain might be due to the development of micro-cracks.

Specimen 6 was first loaded at a tension/compression ratio of 1. Strain gauge readings were taken at load increments of 2 kips. Tension

was then kept constant at 8 kips and the maximum compression reached was 59.4 kips. The load-strain curve was shown in Figure 4.6. It is interesting to note that the load-strain relationship is non-linear even at low compression loads.

5.2.3 Series III

This series consisted of four specimens. The amount of reinforcement was more than that used in the other two series. Ten layers of wire mesh were packed into the thin cement mortar. Figures 4.15 and 4.16, show the typical cracking pattern of the specimens. No visible cracks could be observed until the specimens were near failure. Visible tension cracks, for specimen 7 shown in Figure 4.15, developed at about 3 kips before the specimen failed. The specimen then failed by the crushing of mortar. It is interesting to note that the cracks are smaller and less in number than those in series II, while the failure pattern of the mortar is essentially the same in both series.

The load-strain relationships of the four specimens have been shown in Figures 4.7 to 4.10. The curves all exhibited a similar shape except there were different initial tension strains due to different tension load applied. The compression strains were linear with compression up to about half of the maximum compression that could be resisted by each specimen. Tension was kept constant at 4, 2, 6, 8 kips for specimens 7, 8, 9 and 10, respectively. The maximum compression loads of the specimens were about the same, except for specimen 7 where the maximum compression was 63 kips. No significant interaction between the applied tension and the maximum

compression was observed. The load-tension strain curve of specimen 7 consists of two linear portions with break occurring at load ranging from 20 to 30 kips. Probably this break was due to some micro-cracking developed in the mortar. The load-tension strain curves of specimens 8 and 9 are fairly linear up to a load of 40 kips. The load-tension strain of specimen 10 is non-linear and is quite similar to that of specimen 6. The non-linearity of the curves in both specimens is likely due to the relatively high applied tension which stressed the wire mesh to beyond its proportional limit.

5.3 Modulus of Elasticity

Secant moduli of elasticity at 0.5 maximum compression strength of the specimens under biaxial tension-compression were calculated and presented in Table 4.1. It was observed that the compression load-compression strain curves were linear up to about half of the maximum compressive load that could be reached for each individual specimen. The recommended relationship between the modulus of elasticity and the strength of concrete given by ACI is:

$$E = 57000 \sqrt{f'_c} \qquad (5.1)$$

Using the cylinder strength for each specimen from test results, the corresponding modulus of elasticity was calculated. These recommended values are about 2% to 10% higher than the experimental values. No data was available for specimen 2 because the specimen broke when compression was 18 kips and there were insufficient points

to plot the load-strain curve under biaxial tension-compression. For specimen 5, the difference between the recommended and experimental values is high, about 38%.

Attempts were also made to calculate the modulus of elasticity and Poisson's ratio of the specimens by solving the following two equations at different load levels:

$$\varepsilon_x = \frac{1}{E} [\sigma_x - \nu\sigma_y] \tag{5.2}$$

$$\varepsilon_y = \frac{1}{E} [\sigma_y - \nu\sigma_x] \tag{5.3}$$

Poisson's ratio were found to vary from specimen to specimen, ranging from 0.1 to more than 1. The values of modulus of elasticity calculated using these two equations were even smaller than the secant moduli of elasticity.

5.4 Poisson's Ratio

Attempts were made to find the Poisson's ratio of the specimens from the experimental load-strain curves. The specimens were assumed to behave elastically, homogeneously and isotropically for loads less than 0.5 maximum compression so that the following biaxial stress-strain law was applicable:

$$\varepsilon_x = \frac{1}{E_s} [\sigma_x - \nu\sigma_y] \tag{5.4}$$

Using the above equation, Poisson's ratios at different load levels were calculated for each specimen. The ratios were found to vary from specimen to specimen, ranging from about 0.2 to about 1.0. However, there was no definite variation pattern of the ratios. The Poisson's ratios of most specimens were much higher in comparison with those of concrete which is about 0.2. It was found that the ratios in a specimen were higher when the applied tension was larger.

5.5 General Discussion

This experimental program consisted of ten specimens tested under biaxial tension-compression. The compressive strengths of the specimens in series II and III were quite close to each other except for specimen 7. It appeared that the amount of wire mesh reinforcement had no significant influence on the interaction of tension and compression. If a combined tension-compression strength curve was drawn from the test results, the curve would be a straight line with constant compression being equal to the uniaxial compression strength and dropping to zero when the applied tension approached to the uniaxial tension strength of the specimens.

In this experimental program, a special tension frame was designed as presented in section 3.6. During testing, tension forces transmitted to the bolts were made equal by adjusting the strains in the bolts as close to each other as possible. This could be done by adjusting the degree of tightness of the nuts on the bolts without much problem. The alignment of the bolts could be controlled by using

the wood mould described in section 3.4. It can be concluded that this method employed to transmit tension to the test sections was satisfactory.

During each test, tension and compression strains were measured by both electrical resistance strain gauges and mechanical demec gauges. It was found that the strains obtained from mechanical demec gauges were constantly higher than those obtained from electrical resistance strain gauges and were not presented in this report.

Ultimate strains of the specimens could not be recorded due to the sudden failure of the specimens at maximum compression. From the extrapolation of the compression load-strain curves, it was found that the average ultimate compressive strain was about 0.003 which was equal to the suggested ultimate compressive strain for reinforced concrete.

Chapter VI

SUMMARY AND CONCLUSIONS

6.1 Summary

In this investigation, a brief review of the applications of ferrocement as well as a survey of the various experimental investigations are presented, and ten ferrocement specimens were tested under biaxial tension-compression. Ferrocement is a highly reinforced cement mortar in which the reinforcement consists primarily of layers of wire mesh. The wires of the mesh are usually 0.02 to 0.06 inches in diameter. Since it is possible to cast very thin sections with ferrocement, there are savings in basic materials, namely steel and cement. Early application of ferrocement seemed to be in boat-building and the first application of ferrocement to civil engineering was made by Nervi and Bartoli in the construction of a storage shed. Ferrocement is suitable for cast-in-situ construction and for prefabrication. In some cases of cast-in-situ construction, only a minimum of formwork is required because mortar can be applied directly on the wire mesh. Ferrocement has been used for grain-storage silos, railroad ties, storage tanks for water, milk and liquified gases and underwater structures. It has been suggested for use as a building material in developing countries, especially for roofing of housing construction. A number of investigators have examined the engineering properties of ferrocement such as tensile strength, compressive strength, flexural strength, impact strength and fatigue strength. Tensile strength of ferrocement depends mainly on that of the wire

mesh while compressive strength depends on that of the cement mortar. Conventional reinforced concrete theory can be adopted to predict the flexural strength conservatively until a more reliable theory becomes available.

The behavior of ferrocement under biaxial tension-compression was studied in this program. Special tensile frame was designed to transmit tension through 5/8-in. diameter bolts to the test sections. Compression was applied by using a Baldwin Testing Machine. The principal variables included were the specimen shapes, the amount of wire mesh reinforcement and the values of the applied tension. For each specimen, the tension load was applied to its designated value and was then held constant while compression was increased until failure occurred. Load-strain curves for the specimens were plotted. The behavior of the specimens was discussed with respect to the load-strain relationships and the cracking pattern.

6.2 Conclusions

6.2.1 Conclusions from Various Experimental Investigations

(a) General

Ferrocement is suitable to structures which have strength through forms and structures like silos, water tanks and hanging roofs. Damage due to impact on ferrocement has been found to decrease with increase in specific surface and ultimate strength of the mesh reinforcement. Welded wire mesh is superior compared with other mesh from a uniaxial strength point of view while expanded metal is superior in biaxial loading. The fatigue strength of ferrocement is dependent on the fatigue properties of reinforcement.

(b) Uniaxial tension

(i) Ultimate uniaxial tensile strength of ferrocement is about the same as that of the mesh alone. Orientation of wire mesh has a marked effect on the ultimate tensile strength.

(ii) Tensile stress at first cracking increases linearly with the specific surface ratio of the reinforcement.

(iii) For one type of wire mesh, increasing the specific surface of reinforcement increases the number of cracks to failure, decreases the spacing of cracks and results in finer crack widths.

(iv) Modulus of elasticity and extensibility increase with the steel content. Modulus of elasticity can be conservatively predicted by the law of mixtures of composite materials.

(c) Uniaxial compression

(i) There is no significant increase in the compressive strength with increase in steel content.

(ii) Modulus of elasticity in compression increases directly with increase in steel content.

(iii) For the same steel content, the use of smaller diameter wires will increase the compressive strength and the modulus of elasticity in compression.

(iv) Orientation of the reinforcement has a relatively minor effect in compression compared with its effects in tension and flexure. Lateral reinforcement influences compressive strength much more strongly than longitudinal reinforcement.

(d) Flexure

(i) The behavior of ferrocement elements in flexure is very similar to that of reinforced concrete. Conventional reinforced concrete theory can be used to predict the ultimate bending strength of ferrocement until a more reliable theory becomes available.

(ii) Ultimate flexural strength increases with the steel content. Modulus of elasticity in bending and stress at first cracking increase linearly with increase in steel content. The number of cracks developed increases with an increase in percentage of reinforcement.

(iii) A direct correlation exists between the ultimate flexural strength and a non-dimensional mesh-mortar parameter which takes into account the proportion of mesh wires in the direction of stressing and the strength properties of wire and mortar.

(iv) Orientation of wire mesh has a marked effect on ferrocement reinforced with expanded metal and welded mesh.

(v) Increase in specific surface of reinforcement will increase the moment at first crack and the number of cracks, but decreases the crack width for a given steel content.

(vi) For the same steel content, modulus of elasticity and bending strength are slightly greater when smaller diameter wires are used.

(vii) Moment at first crack in flexure depends on the area of reinforcement, thickness of specimen, proof stress of reinforcement and modulus of elasticity of the composite material.

6.2.2 Conclusions from Experimental Results

From the test results, it appears that there is no significant interaction between the tension and compression for the specimens tested. The amount of wire mesh does not influence the interaction significantly. A tension-compression strength curve drawn from the test results would be a straight line with constant compression almost equal to the uniaxial compressive strength and then dropping to zero as tension approaching to the uniaxial tensile strength of the specimens. The load-compressive strain curves under biaxial tension-compression are fairly linear up to 0.5 ultimate compressive load. The ultimate compressive strain was found to be about 0.003.

The average secant modulus of elasticity at 0.5 ultimate compressive strength was found to be about 4.2×10^6 psi which was smaller than the value calculated according to the ACI code suggested for a reinforced concrete member. The values depend on the Poisson's ratio effect and the ratio of the stresses in both the longitudinal and lateral directions. Attempts have been made to calculate the Poisson's ratio of ferrocement under combined tension-compression. It was assumed that the specimens were homogeneous, and behaved isotropically and elastically for loads less than half of the maximum compressive strength. However, the values calculated varied from specimen to specimen and there was no significant pattern of variation. A further testing program would be required for a better understanding of the behavior of ferrocement under combined tension and compression.

REFERENCES

1. Nervi, P.L., "Ferrocement: Its Characteristics and Potentialities", Cement and Concrete Association, London, England, Library Translation #60, 1956.

2. Nervi, P.L., "Structures", Translated from Italian by Giuseppina and Mario Salvadori, F.W. Dodge Corporation, New York, 1956, pp. 50-62.

3. Cassie, W.F., "Lambot's Boats: A Personal Rediscovery", Journal of Concrete Society, Cement and Concrete Association, Vol. 1, No. 11, Nov. 1967, pp. 380-382.

4. Abercrombie, S., "Ferrocement: Building with Cement, Sand and Wire Mesh", Schocken Books Inc., United States, 1977.

5. Shah, S.P., "New Reinforcing Material in Concrete", Journal of American Concrete Institute, May 1974, pp. 257-262.

6. Kelly, A.M. "Ferrocement as a Fishing Vessel Construction Material", Montreal, Conference on Fishing Vessel Construction Materials, October 1968, sponsored by Federal Provincial Atlantic Fisheries Committee, pp. 135-162.

7. Hagenbach, T.M., "Ferrocement Boats", Montreal Conference on Fishing Vessel Construction Materials, Canadian Fisheries Reports No. 12, June 1969.

8. Bezukladov, V.F., et al., "Ship Hulls made of Reinforced Concrete", Shipbuilding Publishing House, Leningrad, 1968, English Translation - Navalships Translation (1148) NTIS AD 6800 42.

9. Hurd, M.K., "Ferrocement Boats", ACI Journal, March 1969, pp. 203-204.

10. Jackson, G., "Future with a Promise for Concrete Boat Building", Concrete Construction, Vol. 14, No. 9, 10, Sept. 1969, pp. 344-346 and Oct. 1969, pp. 381-383.

11. Kodar, N.S., "Ferrocement Fishing Trawlers", Indian Concrete Journal, Vol. 45, No. 8, Aug. 1971, pp. 327-328.

12. Thomas, G., "Ferrocement Boats", Indian Concrete Journal, Vol. 45, No. 8, Aug. 1971, pp. 329-332, 354.

13. Baitis, A.E., "Vipers, Ferrocement Planning Boats", Naval Engineering Journal, Vol. 83, No. 2, April 1971, pp. 53-63.

14. "Ferrocement for Canadian Fishing Vessels", Project Report No. 42, compiled and edited by W.H. Scott, Industrial Development Branch, Fisheries Service, Department of Environment, Ottawa, August 1971.

15. Greenius, A.W. and Smith, J.D., "Ferrocement for Canadian Fishing Vessels - Vol. 2", Project Report No. 48, Industrial Development Branch, Fisheries Service, Department of Environment, Ottawa, Jan. 1972.

16. Bigg, W., "An Introduction to Design of Ferrocement Vessel", Report No. 52, Industrial Development Branch, Fisheries Service, Department of Environment, Ottawa, Jan. 1972.

17. "Ferrocement for Canadian Fishing Vessels - Vol. 2", British Columbia Research, Report No. 55, Industrial Development Branch, Department of Environment, Aug. 1972.

18. "Ferrocement for Canadian Fishing Vessels", Report No. 86, Industrial Development Branch, Department of the Environment, Ottawa, March 1975.

19. Samson, J. and Wellens, G., "The Ferrocement Boat", Samson Marine Design Ltd., Lander, B.C., Canada, 1972, 192 pp.

20. Fyson, J., "FAO Investigates Ferrocement Fishing Craft", West Byfleet, Fishing News (Books) Ltd., 1973.

21. Bingham, B., "Ferrocement - Design, Techniques and Application", Cornell Marine Press, Inc., Cambridge, 1974.

22. Dinsenbacher, A.L. and Braver, F.E., "Material Development, Design, Construction and Evaluation of a Ferrocement Planning Boat", Marine Technology, Vol. 11, No. 3, July 1974, pp. 277-296.

23. Alexander, D.J., "Newer Techniques in the Construction of Prestressed Concrete Barges and Prestressed Ferrocement Vessels", Journal of Ferrocement, Vol. 4, No. 6, Oct.-Nov. 1975.

24. Haiduknov, G.K., "Development of Armocement Structures", Bulletin of the International Association for Shell Structures, Dec. 1968.

25. Desayi, P., and Jacob, K.A., "Ferrocement - Its Application in Naval Construction and Civil Engineering", The Indian and Eastern Engineer, Bombay, India, No. 114, 1972, pp. 87-91.

26. "Ferrocement: Applications in Developing Countries", Ad Hoc Advisory Panel of the Board of Science and Technology for International Development, National Academy of Sciences, Washington, D.C., Feb. 1973.

27. Pama, R.P., Lee, S.P. and Vietmeyer, N.D., "Ferrocement, a Versatile Construction Material: Its Increasing Use in Asia", Asian Institute of Technology (Bangkok), 1976. (distributed in the United States by the National Academy of Sciences, Washington, D.C.).

28. Shah, S.P. and Aroni, S., "Problems and Prospects for Concrete Housing Construction", Journal of Association of Engineers and Architects in Israel, Vol. 34, No. 2, Feb. 1975, pp. 45-38.

29. Braver, F.E., "State-of-the-Art Survey of Ferrocement", Naval Ship Research and Development Laboratory. Report No. 8-529, January 1971, Maryland 21402.

30. Walkus, R. and Kowalski, T.G., "Ferrocement: A Survey", Journal of the Concrete Society, Vol. 5, No. 2, Feb. 1971, pp. 48-52.

31. Walkus, R., "State of Cracking and Elongation of Ferrocement under Axial Tensile Load", Part I, 1968, Vol. XIV (XVIII) Part II, 1970, Vol. XVI (XX), Buletinul, Institutului Politechnic, Din Iasi.

32. Naaman, A.E. and Shah S.P., "Tensile Test of Ferrocement", Journal of American Concrete Institute, Vol. 68, No. 9, Sept. 1971, pp. 693-698.

33. Shah S.P. and Key, W.H., "Impact Resistance of Ferrocement", Journal of Structural Division, A.S.C.E., Jan. 1972.

34. Shah, S.P., "Evaluation of Ferrocement as a Construction Material", Proceedings of the Conference on New Materials in Concrete Construction, held at University of Illinois, Chicago, Dec. 1972.

35. Shah, S.P. and Key, W.H., "Ferrocement as a Material for Offshore Structures", Offshore Technology Conference, Proceedings, Houston, April 1971, Paper No. 1465.

36. Desayi, P., and Jacob, K.A., "Strength and Behavior of Ferrocement in Tension and Flexure", Proceedings Symposium on Modern Trends in Civil Engineering, Roorkee, India, Vol. 1, 11-13, Nov. 1972, pp. 274-279.

37. Pama, R.P., Sutharatanachaiyaporn, C. and Lee, S.L., "Rigidities and Strength of Ferrocement", First Australian Conference on Engineering Materials, University of New South Wales, Aug. 26-28, 1974.

38. Nathan, G.K. and Paramasiva, P., "Mechanical Properties of Ferrocement Materials", First Australian Conference on Engineering Materials, University of New South Wales, Aug. 26-28, 1974, pp. 309-331.

39. Nathan, G.K., Paramasiva, P., "Tensile and Flexural Cracking Stress of Ferrocement", Engineering Journal of Singapore, Vol. 3, No. 1, 1976.

40. Johnston, C.D. and Matter, S.G., "Ferrocement Behavior in Tension and Compression", Journal of Structural Division ASCE, Vol. 102, No. 5, May 1976.

41. Rao, K. and Gowder, K., "Behavior of Ferrocement in Direct Compression", Cement and Concrete (New Delhi), Vol. 10, No. 3, Oct. 1969, pp. 231-237.

42. Collen, L.D.G. and Kiwan, R.W., "Some Notes on the Characteristics of Ferrocement", Civil Engineering and Public Works Review, London, England, Vol. 54, No. 631, Feb. 1959, pp. 195-196.

43. Chang, W.F., "Flexural Behavior of Ferrocement Panels", ASCE, Proceedings of Civil Engineering in Oceans, Dec. 10-12, 1969, pp. 1023-1044.

44. Muhlert, H.F., "Analysis of Ferrocement in Bending", Department of Naval Architect and Marine Engineering, University of Michigan, Report 043, Jan. 1970.

45. Rao, K.A. and Gowder, C.S.K., "A Study of the Behavior of Ferrocement in Flexure", Indian Concrete Journal, Vol. 45, No. 4, April 1971, pp. 178-183.

46. Logan, D., and Shah, S.P., "Moment Capacity and Cracking Behavior of Ferrocement in Flexure", Journal of American Concrete Institute, Proceedings, Vol. 70, No. 12, Dec. 1973, pp. 799-804.

47. Rajagopalan, K. and Parameswaran, V.S., "Cracking and Ultimate Strength Characteristics of Ferrocement in Direct Tension and in Pure Bending", Indian Concrete Journal, Vol. 48, No. 12, Dec. 1974, pp. 387-393.

48. Rajagopalan, K. and Parameswaran, V.S., "Analysis of Ferrocement Beams", Journal of Structural Engineering, Vol. 2, Jan. 1975, pp. 155-164.

49. Johnston, C.D. and Mowat, D.N., "Ferrocement - Material Behavior in Flexure", Journal of the Structural Division, ASCE, Vol. 100, No. 10, Oct. 1974, pp. 2053-2069.

50. Surya Kumar, G.V. and Sharma, P.C., "An Investigation into the Flexural Behavior of Ferrocement", Journal of Structural Engineering, Vol. 2, Jan. 1975, pp. 137-144.

51. Kumar, G.V. and Sharma, P.G., "An Investigation of the Ultimate and First Crack Strengths of Ferrocement in Flexure", Indian Concrete Journal, Nov. 1976, pp. 335-340, 344.

52. Shah, S.P., Naaman, A.E. and Balaguru, P.N., "Analysis and Behavior of Ferrocement in Flexure", Journal of Structural Division, ASCE, Vol. 103, No. 10, Oct. 1977, pp. 1937-1951.

53. Picard, A. and Lachance, L., "Preliminary Fatigue Tests on Ferrocement Plates", Cement and Concrete Research, Vol. 4, No. 6, Nov. 1974, pp. 967-978.

54. McKinnon, E.A. and Simpson, M.G., "Fatigue of Ferrocement", Journal of Testing and Evaluation, Vol. 3, No. 5, Sept. 1975, pp. 359-363.

55. P. Karasudhi, A.G. Mathew and P. Nimityongskul, "Fatigue of Ferrocement in Flexure", Journal of Ferrocement, Vol. 7, No. 2, October 1977, pp. 81-95.

56. Viswanath, T., Mhatre, R.P. and Seetharamulu, K., "Test of a Ferrocement Precast Folded Plate", Journal of Structural Division, ASCE, Vol. 91, No. 6, Dec. 1965, pp. 239-249.

57. Gopalakrishnan, R.J., "Ultimate Moment and Flexural Rigidity of Ferrocement Folded Plate Beams", Proceedings, Symposium on Ultimate Load Design of Concrete Structures, P.S.G. College of Technology, Coimbatore, 1967, Section II, pp. 83-89.

58. Desayi, P. and Joshi, A.D., "Ferrocement Load-bearing Wall Elements", Journal of Structural Division, ASCE, Vol. 102, No. 9, Sept. 1976, pp. 1903-1916.

59. Chang, W.F., "Properties and Costs of Ferrocement and Fibreglas Composite Panels", Composite Materials in Engineering Design, Symposium, 6th Proceedings, Washington University, St. Louis, May 11-12, 1972, pp. 93-97.

60. Khan, L.F., Townsend, W.H. and Kaldjian, M.J., "Ferrocement Steel-Plate Composite Beams", Journal of American Concrete Institute, Vol. 72, No. 3, March 1975, pp. 94-97.

61. Kowalski, T.G., "Ferrocement Marine Mixes in a Warm and Humid Environment", Concrete Sea Structure, Symposium, Proceedings, Tibilisi, Georgian, S.S.R., Sept. 26-30, 1972, pp. 150-158.

62. Moan, T., "On Shell Effects on Ferrocement Vessels", Norweigan Maritime Research, Vol. 1, No. 4, 1973, pp. 1-6.